Quaternary Science Reviews 288 (2022) 107594

Contents lists available at ScienceDirect

Quaternary Science Reviews

journal homepage: www.elsevier.com/locate/quascirev

A Middle Pleistocene *Coelodonta antiquitatis praecursor* Guérin (1980) (Mammalia, Perissodactyla) from Les Rameaux, SW France, and a revised phylogeny of *Coelodonta* Bronn, 1831

Antigone Uzunidis [a, *], Pierre-Olivier Antoine [b], Jean-Philip Brugal [c]

[a] Institut Català de Paleoecologia Humana i Evolució Social (IPHES-CERCA), Zona Educacional 4, Campus Sescelades URV (Edifici W3), 43007, Tarragona, Spain
[b] Institut des Sciences de l'Évolution de Montpellier, Univ Montpellier, CNRS, IRD, Place Eugène Bataillon, 34095, Montpellier, Cedex 05, France
[c] Aix-Marseille Université, CNRS, Minist Culture, UMR 7269 LAMPEA, CS 90412, F-13097, Aix-en-Provence, France

ARTICLE INFO

Article history:
Received 27 February 2022
Received in revised form
11 May 2022
Accepted 30 May 2022
Available online xxx

Handling Editor: Danielle Schreve

Keywords:
Morphometric analyses
Phylogenetic analysis
Evolution
Historical biogeography
Pleistocene
Eurasia
Coelodonta

ABSTRACT

In recent years, the evolutionary history of rhinoceroses has been extensively developed and clarified, notably with the help of morpho-anatomical and molecular-based phylogenetic analyses. Within Rhinocerotidae, the genus *Coelodonta* Bronn, 1831, is one of the most representative icons of the Ice Ages, ranging from the Late Pliocene to the latest Pleistocene. Nevertheless, few studies have focused on its phylogeny and the systematic assignment of its Middle Pleistocene representatives is fervently debated. Indeed, the earliest European specimens of *Coelodonta* are considered as documenting either *C. tologoijensis* Belyaeva in Vangengejm et al., 1966), of Russian affinities, or an early subspecies of *Coelodonta antiquitatis* (Blumenbach, 1799), *C. a. praecursor* Guérin1980. Accordingly, *C. antiquitatis* would then first occur in the Late Pleistocene or in the Middle Pleistocene depending on the hypothesis. The current work aims to describe and identify cranio-mandibular and postcranial remains of *Coelodonta* from the Middle Pleistocene Les Rameaux locality, SW France, and to compare them with all Eurasian representatives of the genus, including the oldest European specimens from Bad Frankenhausen. A combination of morphometric and morpho-anatomical phylogenetic analyses strongly supports *C. a. praecursor* and *C. a. antiquitatis* as distinct and valid subspecies and allows for the refutation of the taxonomic assignment of the Bad Frankenhausen skull to *C. tologoijensis*. This work proposes the first comprehensive phylogeny for *Coelodonta*, further tracing its biogeographical history.

1. Introduction

Like mammoths, rhinoceroses of the genus *Coelodonta* Bronn, 1831 are emblematic flagships of the Pleistocene megafauna of the northern hemisphere (Guthrie, 1990; Kahlke, 1999, 2014). Indeed, the woolly rhinoceros *Coelodonta antiquitatis* is one of the first fossil species ever recognized and described by Blumenbach (1799), for a long time restricted to this species. It became extinct after the last glacial maximum, by the latest Pleistocene (Orlova et al., 2004; Stuart and Lister 2007; Kuzmin, 2010). It was only in the 1960s that two new species were described: one from the Early-Middle Pleistocene of northeastern Russia (*Coelodonta tologoijensis* Belyaeva in Vangengejm et al., 1966) and the other one from the Early Pleistocene of North China (*Coelodonta nihowanensis* Kahlke, 1969). In 2011, the oldest undisputable representative of the genus, *Coelodonta thibetana* Deng et al., (2011), was described in the Zanda Basin, from upper Pliocene deposits of southwestern Tibet (Deng et al., 2011).

In the meantime, Guérin (1980) had suggested splitting *C. antiquitatis* into two chrono-subspecies, with a Middle Pleistocene form named *C. a. praecursor* being more slender and higher than the Late Pleistocene nominal subspecies, *C. a. antiquitatis*. This distinction would further match a general trend within the species, from cursorial to fully graviportal locomotor adaptations. Ever since, *Coelodonta a. praecursor* was described in several European sites, notably characterized by the slenderness of postcranial limb bones. This subspecies was reported in France at La Fage (type locality of the sub-species, MIS 10/8; Guérin, 1973, 1980), Romain-la-Roche (MIS 6; Guérin, 2010), Coudoulous II (MIS 6; Uzunidis and

* Corresponding author.
E-mail address: antigone.uzunidis@wanadoo.fr (A. Uzunidis).

https://doi.org/10.1016/j.quascirev.2022.107594
0277-3791/

Brugal, 2018) and Greece, at Gephyra (Pleistocene; Tsoukala, 1991), although the latter assignment has recently been challenged (Giaourtsakis, 2022).

Kahlke and Lacombat (2008) described the earliest *Coelodonta* skull from Western Europe (Bad Frankenhausen, Germany, MIS13/12) as documenting *C. tologoijensis*. In their opinion, there is no significant difference between the concerned specimen and the skull from La Fage. Accordingly, they considered *Coelodonta antiquitatis praecursor* Guérin (1980) to be a junior synonym of *Coelodonta tologoijensis* Belyaeva in Vangengejm et al., 1966). In the meantime, Guérin (2010) argued that the morphological differences between *Coelodonta* of Bad Frankenhausen and La Fage, on the one hand, and the archetypical *Coelodonta antiquitatis antiquitais*, on the other hand, were insufficient to justify the existence of two distinct species. He therefore proposed to maintain both entities as formal subspecies (*C. a. praecursor* and *C. a. antiquitatis*) within *C. antiquitatis*, and to further consider the Bad Frankenhausen skull as documenting *C. a. praecursor* (Guérin, 2010).

Since 2010, this taxonomic issue has not been re-evaluated and very little is known about the distribution of *Coelodonta* in Europe, notably in the absence of a strong consensus concerning the Middle–Late European rhinoceros record (e. g. Kahlke et al., 2011; Álvarez-Lao and Garcia, 2011). Moreover, the phylogenetic relionships of *Coelodonta* have been extensively studied in the last years based on molecular markers (DNA, proteins; see Liu et al., 2021 and references therein), but only a few morphoanatomy-base work have investigated the phylogenetic affinities of *Coelodonta* (e.g., Antoine, 2002; Deng et al., 2011; Antoine et al., 2022) since the pioneering studies of Groves (1983) and Cerdeño (1995). The present study aims to i) describe the well-preserved skull of *Coelodonta* found at Les Rameaux, Middle Pleistocene, SW France, ii) propose a comprehensive morphoanatomical and metric comparison within *Coelodonta*, iii) perform a taxonomically-exhaustive computerized phylogeny of this genus, in order to iv) test the validity of all species and subspecies previously defined within *Coelodonta*; v) clarify the taxonomic assignment of the Bad Frankenhausen skull, and vi) propose a phylogenetically-constrained scenario for the historical biogeography of *Coelodonta*.

2. The Les Rameaux locality

The Les Rameaux locality (Saint-Antonin-Noble-Val, Tarn-et-Garonne Department) is situated in a karstic cavity with a vertical entrance, located at the border of a limestone plateau overhanging the Aveyron River (Fig. 1). Excavations undertaken between 1985 and 1991 yielded an abundant and species-rich fossil material (Rouzaud et al., 1990). Two main chambers are distinguished, one being dominated by herbivore remains ("Amont" i.e. upstream) and the other one by carnivores ("Aval" i.e. downstream), whereas older deposits are present in the upper part of the cavity. The fossil assemblage dates back to the Late Middle Pleistocene, and bone accumulation is likely to result from several distinct events. Taphonomical analyses strongly suggest a natural accidental origin for the ungulate accumulation in the Amont area (Coumont, 2006), and the use of the cavity as den or lair for the Aval area (then with a different horizontal entrance presently closed). A preliminary faunal list includes nine herbivore, eight carnivore, and a dozen meso- and micromammalian species; horses are dominant over other ungulates in the Amont area whereas wolf, cave hyena, and cave lion are the most abundant species in the Aval area. Lastly, the Amont area yields a small lithic artefact series (n = 76), essentially made out of quartz (with choppers and chopping tools) attributed to an older phase of the Middle Palaeolithic, which likely points to the presence of controlled and active scavenging from natural bone accumulation (Brugal and Jaubert, 1991).

From its discovery onward, several specific studies have been conducted on the Les Rameaux material, allowing us to refine taxonomic assignments and to provide a general biochronological context. The site yields the cervid *Haploidoceros mediterraneus*, first described in the Middle Pleistocene Lunel-Viel locality (Hérault; Bonifay, 1967; Croitor et al., 2008) and dated to the MIS 7 (Brugal et al., 2021). This cervid is also found in the MIS 5 Spanish sites of Cova del Rinoceront and Preresa (Daura et al., 2015; van der Made and Mazo, 2014–2015). Horse remains (ñ850) are represented by all skeletal elements and referred to as *E. caballus mosbaschensis* (Uzunidis-Boutillier, 2017). The morphometrical analysis of the wolves brings them closer to the small *Canis lupus lunellensis* from Lunel-Viel (Boudadi-Maligne, 2010, 2012). A large sample of cave lion *Panthera* (*Leo*) (MNI ≈33) shows body sizes intermediate between the two chronologically-distinct forms *P.* (*L.*) *spelaea fossilis* and the more recent *P.* (*L.*) *spelaea spelaea* (Argant and Brugal, 2017); accordingly, this sample typifies a new subspecies named *Panthera spelaea intermedia. Hyaena prisca*, present at Les Rameaux, is also commonly found at Lunel-Viel and some coeval sites (Es-Taliens, Escale, Montsaunès, or Montmaurin; Bonifay, 1971). Glires, especially rodents, provide complementary information with the latest Middle Pleistocene age suggested by the enamel thickness on *Arvicola cantiana* teeth (Jeannet, 2005; Jeannet and Mein, 2016). The Les Rameaux rabbit is similar to those of Lunel-Viel and Orgnac III, both dated to the latest Middle Pleistocene (Pelletier, 2018). The two species of *Lepus* (*L. timidus* and *L. granatensis*) are also recorded at Les Rameaux for the only occurrence of the latter in southern France.

Les Rameaux is a complex karstic site documenting several biological events that contribute to distinct fossil accumulations. The mammal assemblages are species-rich and their evolutionary stage clearly indicates a late Middle Pleistocene age, with some evidence of climatic variations, from relatively cool to temperate conditions throughout the sequence. It still remains difficult to specify exactly the period covered by the entire filling, and we can hypothesize a time period ranging from MIS 9 to MIS 6, more probably around MIS 7 and 6. Due to their large size, the rhino remains from Les Rameaux, especially the skull, have remained blocked in the vertical conduit leading to the Amont area, and they can be unambiguously associated with the mammal collection from this very area.

3. Material and methods

Abbreviations: Capital letters are used for upper teeth (I, C, D, P, M), and lower-case letters for lower teeth (i, c, d, p, m). McII, McIII, and McIV stand for second, third, and fourth metacarpals, respectively. The cranio-mandibular, dental, and postcranial terminology is that of Heissig (1972: pl. 13) and Antoine (2002) for rhinocerotids.

3.1. Morphometrical analysis

The Les Rameaux sample has been metrically and morphologically compared to the Middle and Late Pleistocene populations identified as *Coelodonta antiquitatis praecursor*, *Coelodonta antiquitatis* and *Coelodonta tologoijensis* (Fig. 1; Table 1).

Measurements were taken with a caliper and are all expressed in millimeters. Linear measurements on the skull (Fig. 2) were taken following Guérin (1980: Fig. 4) and the angle on the skull from Kahlke and Lacombat (2008: Fig. 4). Dental measurements (Fig. 2) are length (L) and width (w) taken at the base of the crown following the recommendations of van der Made (2010).

The relative proportions of cranial and dental elements were analyzed using log-ratio diagrams (Simpson, 1941). This type of graph allows the comparison of differences in size and

Fig. 1. Location map of the Les Rameaux locality (late Middle Pleistocene, SW France) and other Middle and Late Pleistocene *Coelodonta* samples used for comparison in this study. [Full width suggested].

Table 1
Middle and Late Pleistocene *Coelodonta* samples compared to the one from Les Rameaux in this study. Type localities for *C. tologoijensis* and *C. antiquitatis praecursor* appear in grey.

Locality	Species	Chronology	Author(s)
Zasukhino 2, Russia	*C. tologoijensis*	Early Pleistocene (~1.8 Ma)	Kahlke (1994); Alexeeva and Erbajeva (2005)
Ust-Obor, Russia	*C. tologoijensis*	Early Pleistocene (~1.4 Ma)	Kahlke (1994); Alexeeva and Erbajeva (2005)
Zasukhino 3, Russia	*C. tologoijensis*	Late Early Pleistocene (0.9 Ma)	Alexeeva and Erbajeva (2005)
Nalaikha, Mongolia	*C. tologoijensis*	Early Pleistocene (>0.9 Ma)	Eisenmann and Kuznetsova (2004)
Tologoi 2.5, Russia (type locality)	*C. tologoijensis*	Early Middle Pleistocene (~0.6 Ma)	Vangengejm et al. (1966); Alexeeva and Erbajeva (2005)
Bad Frankenhausen, Germany	*C. tologoijensis*	MIS 12 (~0.45 Ma)	Kahlke and Lacombat (2008)
La Fage, France (type locality)	*C. a. praecursor*	MIS 8 (~0.27 Ma)	Guérin (1973)
Les Rameaux, France	*C. a. praecursor*	late Middle Pleistocene	This study
Neumark-Nord, Germany	*C. antiquitatis*	MIS 7 (~0.20 Ma)	Van der Made, 2010
Coudoulous II l.9, France	*C. a. praecursor*	MIS 6 (~0.16 Ma)	Uzunidis-Boutillier (2017); Uzunidis and Brugal (2018)
Romain-la-Roche, France	*C. a. praecursor*	MIS 6 (~0.16 Ma)	Guérin (2010)
Arroyo Culebro, Spain	*C. antiquitatis*	Late Pleistocene	Arsuaga and Aguirre (1979); Álvarez-Lao and García, 2011
Ajoie, Switzerland	*C. antiquitatis*	MIS 4–3 (0.07–0.03 Ma)	Becker et al. (2015)
Jaurens, France	*C. a. antiquitatis*	MIS 3 (~0.050 Ma)	Guérin (1983)

conformation between several samples based on scaled measurements on a reference series. In this study, we used *C. nihowanensis* as an outgroup and used measurements published by Qiu et al. (2004) for upper and lower teeth and Deng et al. (2011) for the skull.

3.2. Parsimony analysis

The parsimony analyses were performed through 282 craniomandibular, dental, and postcranial characters. The 278 first characters derive from those of Antoine et al. (2022), adapted to Rhinocerotinae and implemented from a proven matrix by Antoine (2002, 2003), more focused on Elasmotheriinae among Rhinocerotidae. The characters 279–281 of the current matrix correspond to the characters 42–44 of Deng et al.'s (2011) analysis devoted to *Coelodonta thibetana*. The character 282 is new (Humerus: fossa olecrani (shape): 0, symmetric; 1, laterodistally pinched).

All multistate characters were treated as additive, except for the characters 66, 87, 95, 129, 177, and 263 (non-additive).

As in Antoine (2002) and subsequent analyses, the outgroup includes the living Brazilian tapir *Tapirus terrestris*, the early non-rhinocerotid rhinocerotoid *Hyrachyus eximius*, and two Paleogene stem rhinocerotids (*Trigonias osborni* and *Ronzotherium filholi*). Aside from the outgroup, we have used a branching group (Antoine, 2002, 2003; Orliac et al., 2010; Boivin et al., 2019; Antoine et al., 2022), consisting of a selection of representatives of suprageneric groups documenting non-Rhinocerotina Rhinocerotidae: Elasmotheriinae (*Subhyracodon occidentalis*), stem Rhinocerotinae (*Plesiaceratherium mirallesi*), Aceratheriini (*Aceratherium incisivum*, *Hoploaceratherium tetradactylum*, and *Alicornops simorrense*), and Teleoceratina (*Teleoceras fossiger* and *Brachypotherium perimense*).

The ingroup *sensu stricto* (Rhinocerotina) includes all five living rhinoceros' species (*Rhinoceros unicornis, Rhinoceros sondaicus*, *Dicerorhinus sumatrensis*, *Ceratotherium simum*, and *Diceros bicornis*, i.e. Indian, Javan, Sumatran, white, and black rhinoceroses, respectively). It also comprises a comprehensive sample of 17 extinct species of Neogene and Pleistocene Rhinocerotina*: Lartetotherium sansaniense* (Early to Late Miocene of Europe; Heissig, 2012), *Gaindatherium browni* (Early to Late Miocene of South Asia; Heissig, 1972; Antoine, in press), *Dihoplus schleiermacheri* (Late Miocene of Mediterranean; Heissig, 1999; Pandolfi et al., 2016, 2021a), *Ceratotherium neumayri* (Late Miocene of Mediterranean and South Asia; Heissig, 1999; Antoine and Sarac, 2005*), Stephanorhinus pikermiensis* (Late Miocene of eastern Mediterranean;

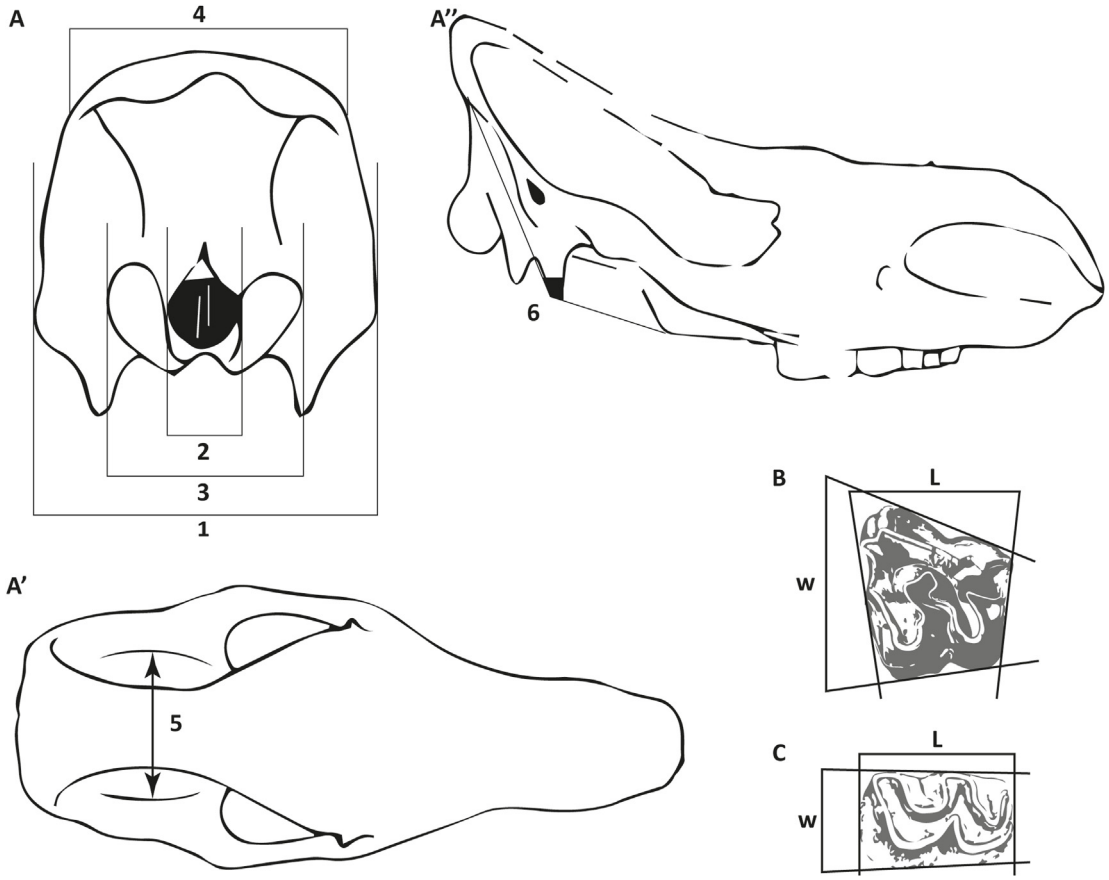

Fig. 2. Protocol used for measuring *Coelodonta antiquitatis* skull and teeth from Les Rameaux. A: nuchal view of the skull: 1 = Width of the skull at the mastoid apophyses; 2 = Width of the foramen magnum; 3 = Width of the occipital condyles; 4 = Width of the occiput. A': Frontal view of the skull: 5 = Minimal width at the postorbital constriction. A'': Lateral view of the skull: 6 = Angle between the base of the skull and the occipital crest. B: Occlusal view of an upper tooth: L = Length and w = width, taken at the neck. C: Occlusal view of a lower tooth: L = Length and w = width taken at the neck. [Full width suggested].

Antoine and Saraç, 2005; Pandolfi et al., 2021a), *Pliorhinus megarhinus* (Latest Miocene to Pliocene of Europe; Pandolfi et al., 2016, 2021b), *Stephanorhinus etruscus* (Late Pliocene to Early Pleistocene of Eurasia; Bourguignon et al., 2016), *Dicerorhinus fusuiensis* (Early Pleistocene of South China and Myanmar; Tong and Guérin, 2009; Yan et al., 2014), *Nesorhinus philippinensis* (early Middle Pleistocene of the Philippines; Bautista, 1995; Ingicco et al., 2018; Antoine et al., 2022), and *Nesorhinus hayasakai* (Early to Middle Pleistocene of Taiwan; Otsuka and Lin, 1984; Antoine et al., 2022). Regarding *Coelodonta*, we have included an exhaustive sample at the species level, namely *Coelodonta antiquitatis* (Middle to Late Pleistocene of Eurasia; Guérin, 1980; van der Made, 2010; Fourvel et al., 2014), *Coelodonta tologoijensis* (Early and Middle Pleistocene of Northeast Asia; Vangengejm et al., 1966; Kalmykov, 2016), *Coelodonta nihowanensis* (Early Pleistocene of China and Mongolia; Qiu et al., 2004; Tong et al., 2011; Tong and Wang, 2014), and *Coelodonta thibetana* (Late Pliocene of Tibet; Deng et al., 2011). In order to test the phylogenetic affinities and taxonomic assignment of late Middle Pleistocene woolly rhinos from Europe, we have first considered *Coelodonta antiquitatis praecursor* from La Fage and Romain-la-Roche (Guérin, 1980, 2010), *Coelodonta tologoijensis* from Bad Frankenhausen (Kahlke and Lacombat, 2008), and the *Coelodonta* from Les Rameaux (Rouzaud et al., 1990; this work) as distinct terminal taxa.

We have scrutinized all available features in the Middle Pleistocene Chinese representatives of *Coelodonta* as listed by Tong (2001: *C. a. chilnesis* Jiang, 1977 and *C. a. venhanensis* Chow, 1979), but also in *C. a. pristinus* Russianov, 1968, *C. a. humilis* Russianov, 1968, and "*C. jacuticus* Lazarev, 2008". This overview allows for invalidating the three later taxa, to be synonymized with the type subspecies (*C. a. antiquitatis*), in good agreement with the conclusions of Shpansky and Boeskorov (2018). On the other hand, both *C. a. chilnesis* Jiang, 1977 (no precise age provided) and *C. a. yenshanensis* Chow, 1979 (fragmentary remains) were described in Chinese only and they are poorly illustrated, which precludes a comprehensive comparison of diagnostic features. Moreover, we had no opportunity to make direct observation of the concerned specimens, for which very few metric data are further available. The concerned analysis therefore encompasses 33 terminal taxa at the species level or below.

The parsimony analyses were achieved through the heuristic search of PAUP 4 3.99.169.0 (Swofford, 2001), with tree-bisection-reconnection (reconnection limit = 8), 1000 replications with random addition sequence (10 trees held at each step), gaps treated as missing, and no differential weighting or topological constraint.

4. Results

4.1. Comparative description

The woolly rhinoceros from Les Rameaux is mostly known through dental and cranial remains (Table 2; Fig. 3), thanks to the discovery of an almost complete skull with an associated mandible. In addition to the teeth embedded in the maxilla and mandible,

Fig. 3. Illustration of a selection of skeletal elements of the Les Rameaux *Coelodonta antiquitatis praecursor*. Due to the fragmentary nature of the skull, it was not possible to fully realize a perfect reconstitution: especially note the uncertain position of frontal part and inclination of the occipital plane. A: Lateral view of the skull and associated jaw (n°17-D2M-503); B: reconstructed left upper toothrow with the M2 (n°111-C2N-53), M1 (n°112-C2N-53), P4 (n°113-C2N-53) and P3 (n°100-C2N-53), occlusal view; C: right upper M2 (n°D-50) and M1 (n°C2M-50), occlusal view; D: right upper M3 (n°34-C10-53), occlusal view; E: reconstructed right lower premolar row with the p4 (n°C1N-50), p3 (n°C1N-50) and p2 (n°C1N-50), lingual view; F: right lower m3 (n°C1N-50), lingual view; G: reconstructed left lower series, with m3 (n°110-B60-53) and m2 (n°40-B6M-53), lingual view. [Full width suggested].

several isolated teeth were found. A total of 18 upper and 22 lower teeth were analyzed belonging to at least three individuals. Contrastingly, the postcranial material is very limited and poorly preserved (only four fragmentary coxal bones and two humerus fragments) and their bad condition discarded further analyses.

4.1.1. Skull

The skull has the archetypical morphological characters of *Coelodonta antiquitatis* (Guérin, 1980, 2010; Antoine, 2002). It is dolichocephalic with a concave dorsal profile and a nasal septum completely ossified, with both horn inserts. The nasal bones are long with the posterior tip of the nasal notch lying above the contact between P4 and M1, as well as being very broad and bending strongly toward the rostral end. The anterior border of the orbits is approximately located above the contact between M2 and M3. Distant crests separate the frontal and parietal bones. However, the postorbital process is absent on the frontal bone whereas it is usually present in Late Pleistocene specimens of *Coelodonta* (Guérin, 1980). On the maxilla, the base of the zygomatic process of the maxillary is low, as observed in the Middle Pleistocene *Coelodonta* (Guérin, 1973, 2010), including the one from Bad Frankenhausen (Kahlke and Lacombat, 2008), contrary to Late Pleistocene individuals (Guérin, 1980). Its development is progressive in the vertical view (sensu Antoine, 2002). The zygomatic arch is low and the postorbital process is absent, as in *Coelodonta* from the Late Pleistocene and the one from Bad Frankenhausen. However, it has been described for the *Coelodonta* of La Fage and Romain-la-Roche (Guérin, 1973, 2010). As in the Bad Frankenhausen skull, the back of the tooth row is located in the posterior half of the skull and much more posteriorly than in Late Pleistocene specimens (Guérin, 1980; Antoine, 2002). On the posterior part of the skull, the occipital crest is straight in the dorsal view. On the squamosal, the temporal crest is present and the area between the temporal and nuchal crest is concave. The articular tubercule of the squamosal bone is smooth while in other specimens of *Coelodonta* it is usually sharp. The transversal profile of the articular tubercle is concave (straight in Late Pleistocene specimens of *Coelodonta*; Guérin, 1980). No posterior groove on the zygomatic process has been observed and the posttympanic process is only slightly developed. The external auditory pseudo-meatus is totally closed. The premaxillae are broken, but there was no alveolus for upper incisors.

4.1.2. Mandible

As for the skull, the associated mandible has the general characteristics of *Coelodonta* (Guérin, 1980; Antoine, 2002). The symphysis is thin and gently sloping up anteriorly. However, the posterior margin of the symphysis is located in front of p2 while it extends generally below the level of p2-p4 in other Late and Middle Pleistocene specimens of *Coelodonta*. The mental foramen is situated in front of p2 and the mandibula one is below the teeth-neckline. On the corpus mandibulae, the lingual groove is absent.

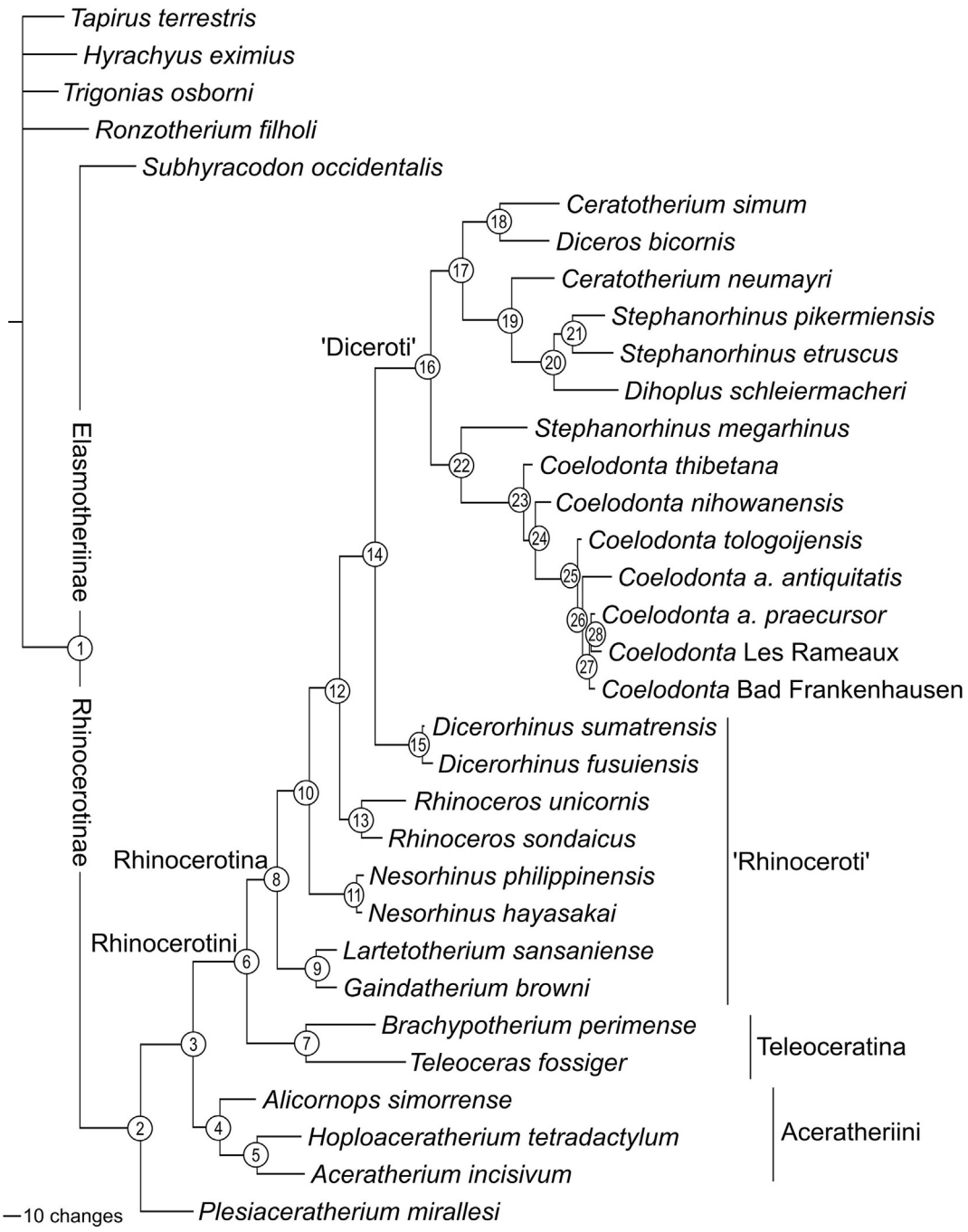

Fig. 4. Phylogram of Rhinocerotina, with a special emphasis on *Coelodonta*. Most parsimonious tree (1349 steps; consistency index = 0.2802; retention index = 0.5409), retrieved from 282 unweighted cranio-mandibular, dental, and postcranial characters scored in 33 tapirid and rhinocerotoid species (see S1 and S2). Node numbers appear in empty circles. [Full width suggested].

The base of this part is very convex as it is for the Late and Middle Pleistocene *Coelodonta* (Guérin, 1980, 2010) and the rhinoceros from Bad Frankenhausen (Kalhke and Lacombat, 2008). It is less convex in *Coelodonta tologoijensis* (Belyaeva in Vangengejm et al., 1966). The ramus is inclined upward and then backward and the coronoid process is well developed. There is no vascular incisure. There are no teeth or their alveoli and the first premolar are absent.

4.1.3. Upper dentition

There is no evidence for the presence of upper incisors or canines (either in the skull or as isolated teeth). In general, the upper cheek teeth are high crowned ("partially hypsodont" sensu Antoine, 2002), with joined roots and characterized by a very corrugated and arborescent enamel covered by cement.

The buccal cingulum is absent on upper premolars. The metaloph and the protocone are never constricted. The protocone and hypocone are joined through a thin lingual wall, in contrast with the usual condition for *Coelodonta* (separated). The hypocone always extends posterior to the metacone. The postfossette is wide and the medifossette always present. The crochet is always present and simple and the crista is always present, except on one P3 (n°53 where there are absent) but this latter condition is probably related

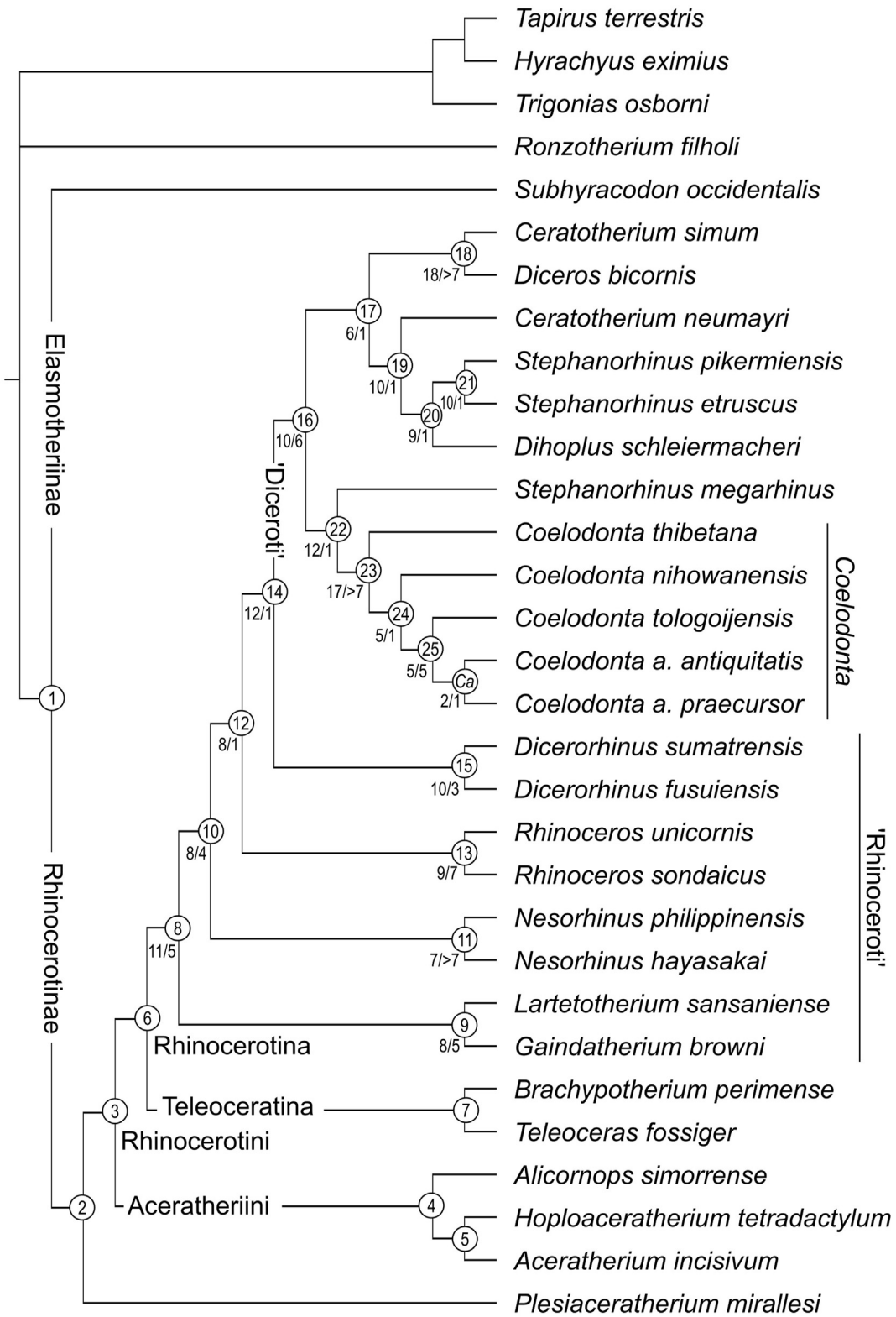

Fig. 5. Phylogenetic relationships of Rhinocerotina, with a special emphasis on *Coelodonta*. Most parsimonious tree (1339 steps; consistency index = 0.2808; retention index = 0.5221), retrieved from 282 unweighted characters scored in 31 tapirid and rhinocerotoid species (see S3 and S4). With respect to Fig. 4, *Coelodonta antiquitatis praecursor* now includes the samples from Bad Frankenhausen and Les Rameaux, hence the lower number of terminals and steps. Node numbers appear in empty circles. Number of unambiguous synapomorphies/Bremer Support are indicated left to Rhinocerotina nodes. [Full width suggested].

Table 2
Coelodonta antiquitatis praecursor (Mammalia, Perissodactyla) from Les Rameaux (Late Middle Pleistocene, SW France): type and number of remains.

Locality	Anatomical element	Left	Right	Unknown	Total
Les Rameaux	Skull	–	–	–	**1**
	Jaw	–	–	–	**1**
	P3	1	1	–	**2**
	P4	3	1	–	**4**
	M1	2	1	–	**3**
	M2	3	2	–	**5**
	M3	2	2	–	**4**
	p2	1	2	–	**3**
	p3	1	2	–	**3**
	p4	1	2	–	**3**
	m1	1	2	–	**3**
	m2	2	2	–	**4**
	m3	3	3	–	**6**
	Humerus	1	–	1	**2**
	Coxal	3	1		**4**
	Innominate	3	1	–	**4**
Total		**24**	**21**	**1**	**52**

to its deep wear. The antecrochet is present on all P4s but not on the P3s (both are usually present in Late Pleistocene specimens of *Coelodonta* (Guérin, 1980).

On upper molars, the buccal and lingual cingula are always absent. The crochet and the crista are always present, except on one M1 (no number), probably due to advanced wear. The antecrochet is absent on one out of three M1s (n° 47), none of the M2s, and on two out of four M3s (n°19 and 34). It is always absent on Late Pleistocene representatives of *Coelodonta* (Guérin, 1980). On the M1-2, the paracone and metacone folds are weakly developed (the metacone fold is absent on M1-2s of Bad Frankenhausen; Kalhke and Lacombat, 2008). The metastyle and metaloph are long and the posterior part of the ectoloph is straight. On the metaloph, the hypocone is sometimes isolated (usually continuous in Late Pleistocene specimens of *Coelodonta*; Guérin, 1980). The protocone is sometimes constricted (M1: n° 112; M2: n° 111 and 77) while it is unconstricted in Late Pleistocene specimens of *Coelodonta* (Guérin, 1980). The posterior cingulum is continuous. On M1, the antecrochet and the hypocone are sometimes joined (usually separated in Late Pleistocene specimens of *Coelodonta*; Guérin, 1980). On M2, the lingual groove of the protocone is always absent. The mesostyle is always strong, as in Middle Pleistocene specimens of *Coelodonta* (Guérin, 1973, 1980, 2010; Kahlke and Lacombat, 2008) and contrary to Late Pleistocene representatives of *Coelodonta* (Guérin, 1980).

The occlusal outline of the M3s is rectangular, the protoloph is transverse, and the posterior groove on the ectometaloph is present. The ectoloph and metaloph are fused (usually distinct in Middle and Late Pleistocene specimens of *Coelodonta*; Guérin, 1980; Kahlke and Lacombat, 2008). The protocone is unconstricted.

4.1.4. Lower cheek teeth

There is no evidence for the presence of any anterior dentition or of permanent first premolars. The lower dental formula is p2-m3. On lower cheek teeth, the external groove is well developed but it is vanishing before the neck. The trigonid is angular and it forms an obtuse angle in occlusal view. The metaconid is constricted and the entoconid joins the hypolophid without a constriction.

On lower premolars, the posterior valley has a V-shaped lingual opening in lingual view, as for *C. antiquitatis* but contrary to *C. tologoijensis* (U-shaped; Belyaeva in Vangengejm et al., 1966). The lingual and labial cingulum are absent. On p2, the paralophid is curved, unconstricted, and simple. The paraconid is developed and the posterior valley is closed lingually on one tooth and open lingually, with a U-shaped opening on the other two (n°4 and 142). The usual pattern in *Coelodonta* is a lingually-open valley in p2s (Guérin, 1980, 2010; Belyaeva in Vangengejm et al., 1966). On lower molars, the hypolophid is oblique and the lingual groove of the entoconid is absent. In general, the lowest points of the two lingual valleys are at the same level in lingual view.

4.2. Metric analysis of cranial and dental remains

In general, the skull is strikingly narrow at the level of the mastoid apophyses and the supraoccipital crest (Table 3; Fig. 6). This is also the case for the Middle Pleistocene *Coelodonta* from La Fage and Bad Frankenhausen (Guérin, 1973; Kalhke and Lacombat, 2008) and the Late Pleistocene *Coelodonta* from Ajoie (Becker et al., 2015), contrary to the skulls from Neumark-Nord, Romain-la-Roche and Jaurens (latest Middle and Late Pleistocene in age, respectively) (Guérin, 1983, 2010; van der Made, 2010). The expression of those two measurements, especially the width of the supraoccipital crest, is impacted significantly by sexual dimorphism with male having wider skulls than females (Puzachenko et al., 2021). Thus, the separation between the specimen may be sex-driven and the narrow skull from Les Rameaux may belong to a female.

The proportion between the breadth of the foramen magnum and the breadth of the condyles between Middle Pleistocene specimens (La Fage, Romain-la-Roche, Les Rameaux, and Bad Frankenhausen) and Late Pleistocene ones (Jaurens, Ajoie, and Arroyo Culebro skull A) differ. In the first group, the width of the condyles is shorter in comparison with the breadth of the foramen magnum while it appears proportionally stronger in the second group specimens. Also, the angulation (Table 3) between the base of the skull and the occipital crest (=112°) suggests a relatively high head carriage, similar to that of the Bad Frankenhausen woolly rhino (=110°) and distinct from that of younger representatives of *Coelodonta* (see Fig. 6 in Kahlke and Lacombat, 2008).

The contour of the upper premolars at the base of the crown is square as in Jaurens or Romain-la-Roche (Fig. 7; Table 4). In Tologoj, on the other hand, they are rectangular (wider jugo-lingually). As for molars, the Tologoj and Les Rameaux samples are morphometrically very close, by being rather longer antero-posteriorly than wide. Lower teeth are particularly small (Table 4), especially the premolars which are sub-square, like their upper counterparts (Fig. 8). However, no particular metric trend seems to stand out

Table 3
Cranial dimensions and angles of *Coelodonta antiquitatis praecursor* from Les Rameaux (this study), "*C. tologoijensis*" from Bad Frankenhausen (Kahlke and Lacombat, 2008), *C. a. praecursor* from La Fage (Guérin, 1973), *C. a. praecursor* from Romain-la-Roche (Guérin, 2010), *C. antiquitaits* from Neumark- Nord van der Made, 2010), *C. antiquitatis* from Arroyo Culebro (Arsuaga and Aguirre, 1979; Álvarez-Lao and García, 2011), *C. antiquitatis* from Ajoie (Becker et al., 2015), *C. a. antiquitatis* from Jaurens (Guérin, 1983) and *Coelodonta nihowanensis* (data from Deng et al., 2011). 1 = Width of the skull at the mastoid apophyses; 2 = Width of the foramen magnum; 3 = Width of the occipital condyles; 4 = Width of the occiput; 5 = Minimal width at the postorbital constriction; Angle = the angle between the base of the skull and the occipital crest. For further detail, see protocol in Fig. 2.

Site	1	2	3	4	5	6
Les Rameaux, France	246	58.96	148	195	128	112
Bad Frankenhausen, Germany	256	57.5	154	184	124.7	110
La Fage, France	248	65	150	–	–	–
Neumark-Nord, Germany	283.7	55.4	154.3	215.5	132.8	–
Romain-la-Roche, France	254.5	64.5	147	198	118	–
Arroyo Culebro, skull A, Spain	300	44	160	250	–	–
Ajoie, Switzerland	236	45	145.5	–	110	–
Jaurens, France	257.5	54	152.5	194	123	–
C. nihowanensis, China	212.5	45	140	145	82.5	–

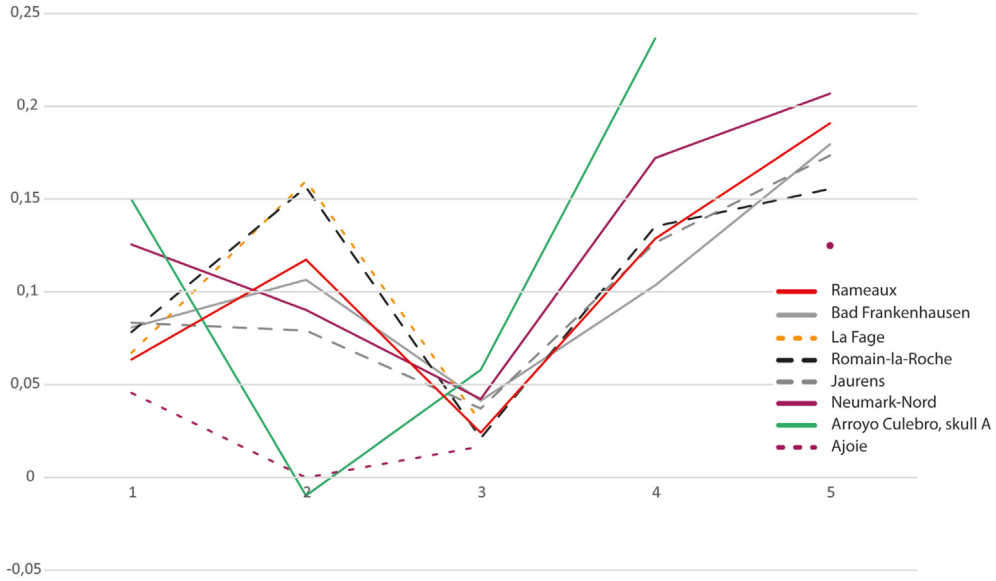

Fig. 6. Ratio diagram (log10) of cranial measurements of *Coelodonta antiquitatis praecursor* from Les Rameaux (this study), "*C. tologoijensis*" from Bad Frankenhausen (Kahlke and Lacombat, 2008), *C. a. praecursor* from La Fage (Guérin, 1973), *C. a. praecursor* from Romain-la-Roche (Guérin, 2010), *C. antiquitaits* from Neumark- Nord van der Made, 2010), *C. antiquitatis* from Arroyo Culebro (Arsuaga and Aguirre, 1979; Álvarez-Lao and García, 2011), *C. antiquitatis* from Ajoie (Becker et al., 2015), and *C. a. antiquitatis* from Jaurens (Guérin, 1983). All values are plotted against the means of *Coelodonta nihowanensis* (data from Deng et al., 2011). 1 = Width of the skull at the mastoid apophyses; 2 = Width of the foramen magnum; 3 = Width of the occipital condyles; 4 = Width of the occiput; 5 = Minimal width at the postorbital constriction. [Full width suggested].

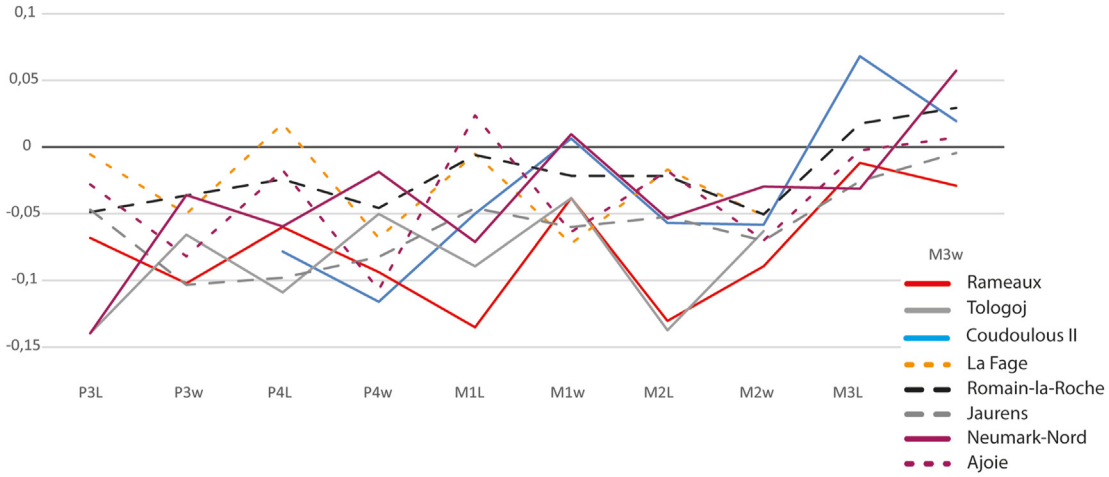

Fig. 7. Ratio diagram (log10) of measurements of upper teeth of *Coelodonta antiquitatis praecursor* from Les Rameaux (this study), *C. tologoijensis* from Tologoj (Belyaeva in Vangengejm et al., 1966), *C. a. praecursor* from La Fage (Guérin, 1973), *C. a. praecursor* from Coudoulous II l.9 (Uzunidis-Boutillier, 2017; Uzunidis and Brugal, 2018) *C. a. praecursor* from Romain-la-Roche (Guérin, 2010), *C. antiquitaits* from Neumark- Nord van der Made, 2010), *C. antiquitatis* from Ajoie (Becker et al., 2015), and *C. a. antiquitatis* from Jaurens (Guérin, 1983). All values are plotted against the means of *Coelodonta nihowanensis* (data from Qiu et al., 2004). Measurements taken at the neck (see methodology): L = length and w = width. [Full width suggested].

though the dimensions of the teeth.

4.3. Phylogenetic analyses

With all 33 terminal taxa included, a single most parsimonious tree is retrieved (length = 1349 steps; consistency index = 0.2802; retention index = 0.5409; Fig. 4; see S1 and S2). Suprageneric relationships within Rhinocerotidae are consistent with those proposed by Antoine (2002, 2003), Antoine et al. (2010, Antoine et al., 2022, Becker et al. (2013), Tissier et al. (2021), and Pandolfi et al. (2021b). Elasmotheriinae and Rhinocerotinae are sister clades (node 1), like Aceratheriini (node 4) and Rhinocerotini (node 3) within Rhinocerotinae, and Rhinocerotina (node 6) and Teleoceratina (node 7) within Rhinocerotini (Fig. 4).

In the next few paragraphs, we will focus on the topology, node support (Bremer Support: BS), and character distribution of the group of interest within Rhinocerotina. The monophyly of 'Rhinoceroti' *sensu* Antoine et al. (2022) is not recovered. This discrepancy is once again related to the fluctuating position of *Dicerorhinus*, depending on the taxonomic samples and proxies used (see discussion in Cappellini et al., 2019; Antoine et al., 2022; Liu et al., 2021; Pandolfi et al., 2021b). Here, 'Rhinoceroti' form a paraphyletic ensemble with four bispecific clades branching successively: the earliest-diverging clade includes *Lartetotherium sansaniense* and *Gaindatherium browni* (node 9), the next is *Nesorhinus* (with *N. philippinensis* and *N. hayasakai*; node 11), the third is

Table 4
Upper and lower tooth dimensions of *Coelodonta antiquitatis praecursor* from Les Rameaux (this study), *C. tologoijensis* from Tologoj (Belyaeva in Vangengejm et al., 1966), *C. a. praecursor* from La Fage (Guérin, 1973), *C. antiquitaits* from Neumark- Nord van der Made, 2010), *C. a. praecursor* from Coudoulous II l.9 (Uzunidis-Boutillier, 2017; Uzunidis and Brugal, 2018), *C. a. praecursor* from Romain-la-Roche (Guérin, 2010), *C. antiquitatis* from Arroyo Culebro (Arsuaga and Aguirre, 1979; Álvarez-Lao and García, 2011), *C. antiquitatis* from Ajoie (Becker et al., 2015) and *C. a. antiquitatis* from Jaurens (Guérin, 1983). Measurements taken at the neck (see methodology): L = length and w = width. For further detail, see protocol in Fig. 2.

Site	Upper teeth										Lower Teeth											
	P3		P4		M1		M2		M3		p2		p3		p4		m1		m2		m3	
	L	w	L	w	L	w	L	w	L	w	L	w	L	w	L	w	L	w	L	w	L	w
Les Rameaux	26.2	37.7	36.2	51.1	41.1	52.1	47.9	47.8		44.6	26.3	17.9	28.8	22.0	36.3	27.0	39.8	30.6	42.7	33.0	48.3	28.5
	42.2	37.7	47.4	30.4	35.1	49.7	46.1	48.8	47.1	52.4	24.3	14.7	31.6	19.7					39.6	25.6	45.8	31.2
			30.6	51.5	37.2	57.3	41.5	57.5	44.0	42.7	25.4	18.9							38.1		48.0	24.1
							41.7	52.1	43.8	46.4											46.6	26.2
							41.4	52.6													39.9	27.4
Tologoj	29	41	34	49	53	54	43	55		53	27	19	30	23	38	27	39	27	50	33	50	31
																	40	28				
La Fage	39	43	47	48	51	49	57	57			31	20	34		41	25	51.5	29	52	33.5		
	40	42	44	46			56.5	56					35	25			50.5	32				
Coudoulous II			36.5	42.1	46.0	58.8	51.8	55.6	62.4	52.3	25.9	19.1	26.9	22.4	39.2	28.8	42.1	31.1			52.9	30.4
l.9													27.2	23.7	42.5	29.9	40.0	28.3			51.3	30.6
													28.7	23.3								
Romain-la-	40	42	45.5	52.5	54	56	61.5	58	58	64.5	28.5	17.5	34	22	43.5	28	49	27	46	31.5	55	32
Roche	40.5	48	38	47.5	50	53.5	59.5	59	56.5	47	29	20	28	24	39	23.5	43	29.5			48.5	28.5
	31	43	40.5	48.5	57	57	52.5	55	52	49	23	18	31.5	29	39.5	24	43					
	31.5	42.5			46.5	54	51	54.5							35	28.5	43.5	31				
					47	55																
Neumark-Nord	29	43.9	38.1	52.7	43.8	59.2	51.2	58.5	48.2	56.8												
							53.2	60.3	51	57.3												
Arroyo Culebro					36		49	62	52	55	29.5	20	37	24.5			52	31	54		55.2	34.2
							46	60	52	56	30	20.5	38.5	26			51.5	30.5	54			
Ajoie	37.5	39.5	42	43	54.5	50	60	56	57	52					37	31	36	30	44	29.5	51.5	31
					54	50	51.5	56.5	55	52.5					32		39	31	47	32.5	53.5	31.5
							57	53	47	48									47	32.5		
							58	51														
Jaurens	39	38.5	40	46	42.5	50.5	55.5	56	52	51	26	18	33.5	21.5	36	23	37	23	49	29	48.5	28
	38.5	39	40.5	44	53	48	56	56	48.5	48	23	17	33	21	43	25.5	37	29	53	32	52	31.5
	39	35	28.5	46	54	52.5	55.5	54.5			28.5	18.5	26	22.5	40	25	50	28.5	48.5	29.5	52	30
	38	40.5	30.5	46	52.5	52	48.5	52			29	19.5			39	25	35	28	45	30	54	32
	25	35			53.5	49.5	46	52			27	16			35	24.5	37	29	47	29		
					53.5	51.5									36.5	25	50	30	53	30.5		
					32	48.5									36	23	45	30				
					30.5	51									43	26.5						

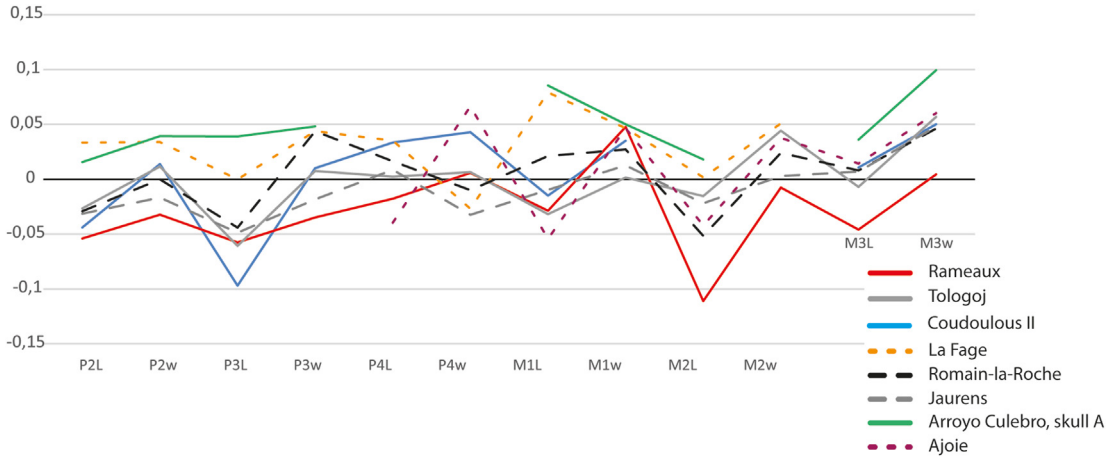

Fig. 8. Ratio diagram (log10) of measurements of lower teeth of the *Coelodonta antiquitatis praecursor* from Les Rameaux (this study), *C. tologoijensis* from Tologoj (Belyaeva in Vangengejm et al., 1966), *C. a. praecursor* from La Fage (Guérin, 1973), *C. a. praecursor* from Coudoulous II l.9 (Uzunidis-Boutillier, 2017; Uzunidis and Brugal, 2018) *C. a. praecursor* from Romain-la-Roche (Guérin, 2010), *C. antiquitatis* from Arroyo Culebro (Arsuaga and Aguirre, 1979; Álvarez-Lao and García, 2011), *C. antiquitatis* from Ajoie (Becker et al., 2015), and *C. a. antiquitatis* from Jaurens (Guérin, 1983). All values are plotted against the means of *Coelodonta nihowanensis* (data from Qiu et al., 2004). Measurements taken at the neck (see methodology): L = length and w = width. [Full width suggested].

Rhinoceros (*R. unicornis* and *R. sondaicus*; node 13), and the fourth is *Dicerorhinus* (*D. sumatrensis* and *D. fusuiensis*; node 15). *Dicerorhinus* is a sister group to the 'Diceroti' (*sensu* Antoine et al., 2022; living African rhinos and their kin; node 16), which are monophyletic and consisting of two clades. The first one gathers the living African rhino clade (*Ceratotherium simum* and *Diceros bicornis*; node 17) as a sister group to a four-species clade with *Ceratotherium neumayri* as a first offshoot (node 19), then *Dihoplus*

schleiermacheri (node 20), and *Stephanorhinus etruscus* plus *S. pikermiensis* (node 21). The second clade within 'Diceroti' places *Pliorhinus megarhinus* as a sister species to *Coelodonta* (node 22; 12 unambiguous cranio-dental and postcranial synapomorphies; BS = 1). The monophyly of *Coelodonta* is strongly supported by 17 unambiguous cranio-mandibular and dental synapomorphies (node 23; BS > 6), with *Coelodonta thibetana* as the first offshoot. *Coelodonta nihowanensis* diverges next. Its clustering with *C. tologoijensis* and *C. antiquitatis* is weakly supported (node 24; BS = 1) despite the presence of five unambiguous cranio-dental synapomorphies. Conversely, the *C. tologoijensis* + *C. antiquitatis* clade is strongly supported (node 25; BS = 5), with the same number of unambiguous cranio-dental and postcranial synapomorphies. The next node groups the highly-divergent *C. antiquitatis* with all Late Middle Pleistocene European representatives of *Coelodonta*. This node 26 is supported by three unambiguous dental synapomorphies (BS = 2). Then, *Coelodonta* from Bad Frankenhausen is sister group to the (*C. a. praecursor*, *Coelodonta* Les Rameaux) clade (node 27; three unambiguous cranial and dental synapomorphies; BS = 1). *Coelodonta* from Bad Frankenhausen is characterized by three unambiguous autapomorphies (protocone and hypocone forming a lingual bridge and protoloph joined to the ectoloph on P2, metacone fold present on M1-2). Ultimately, *Coelodonta* from Les Rameaux clusters with *C. antiquitatis praecursor* with a weak support (node 28; BS = 1) through a single cranial reversal (presence of a postorbital process on the zygomatic arch). *C. a. praecursor* has two unambiguous autapomorphies (tooth row reaching the posterior half of the skull and entoconid unconstricted on lower cheek teeth) and the *Coelodonta* from Les Rameaux five cranio-mandibular and dental autapomorphies (articular tubercle smooth on the squamosal [character subject to changes with ontogeny], posterior margin of the mandibular symphysis in front of p2, lingual wall on P3-4, metaloph and ectoloph fused on M3, and posterior valley lingually closed on p2). These features are variable in *C. antiquitatis* when observed on a comprehensive sample (Guérin, 1980, 2010). We therefore consider that all these morpho-anatomical characters illustrate individual variation.

In order to establish cladistic diagnoses in *Coelodonta* (at the species and subspecies level) and to further test the robustness of the concerned dichotomies, we have performed a second analysis, with *C. antiquitatis praecursor* as a single terminal gathering specimens from Bad Frankenhausen and Les Rameaux, and *C. a. praecursor* (from La Fage and Romain-la-Roche; Guérin, 1980, 2010). This analysis will also be used ultimately for describing the biogeographical history of *Coelodonta*.

Accordingly, the second analysis includes 31 terminal taxa. Again, a single most parsimonious tree is retrieved, with a topology strictly identical to that of the first analysis and similar node supports (length = 1339 steps; consistency index = 0.2808; retention index = 0.5221). Accordingly, we have used the same numbers for the nodes 1–25 (Fig. 5). The most solid nodes among Rhinocerotina are those of living African rhinos (*Ceratotherium simum* + *Diceros bicornis*; 18 unambiguous synapomorphies; BS > 7), *Coelodonta* (17 unambiguous synapomorphies; BS > 7), *Nesorhinus* (seven unambiguous synapomorphies; BS > 7), *Rhinoceros* (nine unambiguous synapomorphies; BS = 7), 'Diceroti' (10 unambiguous synapomorphies; BS = 6), and the (*Coelodonta tologoijensis* + *C. antiquitatis*) clade (five unambiguous synapomorphies, BS = 5). Other nodes have a very low Bremer support (BS = 1–2), despite high numbers of synapomorphies for some nodes, as for the (*Pliorhinus megarhinus* + *Coelodonta*) clade, with 12 unambiguous synapomorphies, or for the nodes involving *Ceratotherium neumayri*, *Dihoplus schleiermacheri*, *Stephanorhinus etruscus*, and *S. pikermiensis* (9–10 unambiguous synapomorphies). This paradox is due to highly homoplastic features occurring among 'Diceroti' and leading to the existence of several distinct tree-islands of similar lengths (see S3 and S4).

In the next few paragraphs, we will focus on the distribution of characters for the (*Pliorhinus megarhinus* + *Coelodonta*) clade and subordinated nodes. The former clade (node 22) is supported by 12 unambiguous synapomorphies, among which the foramen infraorbitalis located above molars, the nasal notch above P4-M1, the external auditory pseudomeatus totally closed, the presence of a crista on P3, the metaloph long on M1-2, the trigonid angular on lower cheek teeth and highly-optimized postcranial features (angle open between the olecranon and the diaphysis on the ulna, posterior McIII-facet absent on the McII, and the Cc2 and Cc3-facets joined on the talus; for details on the latter character, see Antoine, 2002).

Coelodonta (node 23) is characterized by 17 unambiguous synapomorphies, including the nasal horn boss narrow, the anterior border of the orbit above M2-3, the base of the zygomatic process maxillary low, the nuchal tubercle small, the postglenoidal process with a right-angled articulation in cross section, the mandibular symphysis spindly, the premolar row reduced in length with respect to molars, the lingual cingulum always absent on upper cheek teeth, the crochet always present and simple on P2-4, the protocone and hypocone equally developed on P2, the protocone always unconstricted on P3-4, the mesostyle strong on M2, but also the metaconid and the entoconid constricted on lower cheek teeth. The absence of a postcranial features diagnostic for *Coelodonta* is likely related to the absence of the appendicular skeleton assigned to *C. thibetana* (see Deng et al., 2011), leading to ambiguously distributed potential synapomorphies for the concerned anatomical region. *Coelodonta thibetana* is characterized by a mandibular symphysis with a posterior margin in front of p2, a crista usually absent on P3, a protocone always constricted on M1-2, and a metacone fold present on M1-2. Although defined by five unambiguous synapomorphies (nasals with a very broad rostral end and a sagittal ridge on the horn boss, crista always present on upper molars, protocone usually unconstricted and metacone fold absent on M1-2), the clade gathering *C. nihowanensis*, *C. tologoijensis*, and *C. antiquitatis* is weakly supported (node 24; BS = 1). *Coelodonta nihowanensis* is pretty divergent, with eight mandibular, dental, and postcranial unambiguous autapomorphies (mandibular symphysis much upraised, lingual cingulum sometimes absent on D1, protocone and hypocone forming a lingual bridge and protoloph joined to the ectoloph on P2, mesostyle absent on D2, axis-facets sigmoid on the atlas in vertical view, distal side triangular on the pyramidal, and trochlea and distal articulation very oblique on the astragalus). The next node (node 25) places *C. tologoijensis* as a sister species to *C. antiquitatis*, which is supported by five cranio-dental and postcranial unambiguous synapomorphies (nasal septum totally ossified, partial hypsodonty, proximal ulna-facets always fused on the radius, posterior stop absent on the cuboid-facet of the astragalus, and fibula-facet always absent on the calcaneus). Sixteen ambiguous synapomorphies are potentially acquired at this node (cranio-mandibular, dental, and postcranial features). *Coelodonta tologoijensis* is diagnosed by one unambiguous autapomorphy (lingual opening of the posterior valley U-shaped on lower premolars). The *Coelodonta antiquitatis* clade (node Ca) is supported by a posterior valley sometimes closed lingually on p2, an unciform with pyramidal- and McV-facets usually separate, and tibia and fibula in contact or fused along their shafts. The nominal subspecies (*C. a. antiquitatis*) is particularly divergent morpho-anatomically, with one cranial (postorbital process absent on the frontal), twelve dental autapomorphies (crochet usually present and lingual cingulum usually absent on P2-4 and upper molars, antecrochet usually absent on P2-3, P4, and upper molars, D1/P1 always absent, hypocone anteriorly constricted on M1 and

M2, antecrochet sometimes joined to the hypocone on M1, mesostyle weak on M2, and protocone usually unconstricted on M3), and a single postcranial one (limbs shorter and more robust). Its sister subspecies, *C. a. praecursor*, is defined by six cranio-dental autapomorphies (infraorbital foramen located above premolars, base of the zygomatic process maxillary high, postorbital proess present on the zygomatic arch, articular tubercle of the squamosal with a straight profile, protocone unconstricted on M1-2, and entoconid joined to the hypolophid on lower cheek teeth).

4.4. Cladistic diagnoses of Coelodonta and referred species and subspecies

These parsimony analyses (see previous sub-section) allow us to propose the following cladistic diagnoses for all species and subspecies recognized in *Coelodonta*, and also for *Coelodonta* itself (see supplementary information for details on the corresponding characters and character states).

Coelodonta Bronn, 1831: Two-horned rhinocerotines with the nasal horn boss narrow, the anterior border of the orbit located above M2-3, the base of the zygomatic process maxillary low, the nuchal tubercle small, the postglenoidal process with a right-angled articulation in cross section, the mandibular symphysis spindly, the premolar row reduced in length with respect to molars, the lingual cingulum always absent on upper cheek teeth, the crochet always present and simple on P2-4, the protocone and hypocone equally developed on P2, the protocone always unconstricted on P3-4, the mesostyle strong on M2, but also the metaconid and the entoconid constricted on lower cheek teeth. Among "Diceroti", distinct from *Pliorhinus* in having notably a low and thin sygomatic arch, a flat dorsal cranial profile, a nearly horizontal posterior margin on the pterygoid, a low zygomatic/frontal width ratio (less than 1.5), no metaloph constriction on P2-4, lingual cusps most usually separate on P3-4, metacone and hypocone joined on P4, a weak paracone fold on M1-2, lower cheek teeth with a trigonid forming a right dihedron in occlusial view, and a paralophid curved on p2; differing from *Stephanorhinus* in possessing a straight occipital crest in dorsal view, distant posttympanic and paraoccipital processes, a paraoccipital process well developed, no metaloph constriction on P2-4, metacone and hypocone joined on P4, and an external groove vanishing before the neck on lower cheek teeth; different from both *Diceros* and *Ceratotherium* in having a concave cranial dorsal profile, an external auditory pseudo-meatus totally closed (circular), and a small nuchal tubercle.

Coelodonta thibetana Deng et al., 2011: Earliest-diverging representative of *Coelodonta*, with a posterior symphyseal margin in front of p2, a crista usually absent on P3, a protocone always constricted on M1-2, and a metacone fold present on M1-2. Differs from all other − more derived − species of *Coelodonta* in having nasals with a broad rostral end (not very broad) and no sagittal ridge on the horn boss, a crista usually absent on upper molars, a protocone always constricted and a metacone fold present on M1-2. Differs from *C. tologoijensis* and *C. antiquitatis* in having a nasal septum partly ossified and high-crowned teeth but no hypsodonty. Differs from *C. tologoijensis* in possessing a V-shaped lingual opening of the posterior valley in lower premolars, in lingual view. Further differs from *C. antiquitatis* in bearing a posterior valley always open lingually on p2.

Coelodonta nihowanensis Kahlke, 1969: Early representative of *Coelodonta*, with a mandibular symphysis much upraised, a lingual cingulum sometimes absent on D1, protocone and hypocone forming a lingual bridge and protoloph joined to the ectoloph on P2, a mesostyle absent on D2, axis-facets sigmoid on the atlas in vertical view, a distal side triangular on the pyramidal, and trochlea and distal articulation very oblique on the astragalus. Differs from *C. thibetana* in having nasals with a very broad rostral end and a sagittal ridge on the horn boss, a crista always present on upper molars, a protocone usually unconstricted and a metacone fold absent on M1-2. Differs from *C. tologoijensis* and *C. antiquitatis* in having a nasal septum partly ossified, high-crowned teeth but no hypsodonty, proximal ulna-facets usually separate on the radius, a posterior stop present on the cuboid-facet of the astragalus, and a fibula-facet always present on the calcaneus. Differs from *C. tologoijensis* in possessing a V-shaped lingual opening of the posterior valley in lower premolars, in lingual view. Further differs from *C. antiquitatis* in bearing a posterior valley always open lingually on p2, an unciform with pyramidal- and McV-facets always separate, and tibia and fibula independent.

Coelodonta tologoijensis Belyaeva in Vangengejm et al., 1966: Sister species of *C. antiquitatis*, defined by a lingual opening of the posterior valley U-shaped on lower premolars. Differs from *C. thibetana* in having nasals with a very broad rostral end and a sagittal ridge on the horn boss, and a mandibular symphysis with a posterior margin at the level of p2-4. Differs from *C. nihowanensis* in possessing a mandibular symphysis much upraised, lingual cingulum sometimes absent on D1, and a mesostyle present on D2. Further differs from *C. antiquitatis* in having a posterior valley always open lingually on p2, an unciform with pyramidal- and McV-facets always separate, and tibia and fibula independent.

Coelodonta antiquitatis Blumenbach, 1799: Most derived species of *Coelodonta*, with a posterior valley sometimes closed lingually on p2, an unciform with pyramidal- and McV-facets usually separate, and tibia and fibula in contact or fused along their shafts. Differs from *C. thibetana* in having a mandibular symphysis with a posterior margin at the level of p2-4, a crista always present on P3, a protocone usually unconstricted on M1-2, and a metacone fold absent on M1-2. Differs from *C. nihowanensis* in possessing a nasal septum totally ossified, a mandibular symphysis nearly horizontal, cheek teeth partially hypsodont, a lingual cingulum present on D1, protocone and hypocone usually separate and protoloph usually disconnected from the ectoloph on P2, a mesostyle present on D2, axis-facets sigmoid on the atlas in vertical view, proximal ulna-facets always fused on the radius, a distal side elliptic on the pyramidal, a posterior stop absent on the cuboid-facet and trochlea and distal articulation in the same axis on the astragalus, and a fibula-facet always absent on the calcaneus. Further differs from its sister species *C. tologoijensis* in possessing a V-shaped lingual opening of the posterior valley in lower premolars, in lingual view.

Coelodonta antiquitatis Blumenbach, 1799: Most derived representative of *Coelodonta*, with a postorbital process absent on the frontal, a crochet usually present and a lingual cingulum usually absent on P2-4 and upper molars, an antecrochet usually absent on P2-3, P4, and upper molars, D1/P1 always absent, a hypocone anteriorly constricted on M1 and M2, an antecrochet sometimes joined to the hypocone on M1, a mesostyle weak on M2, a protocone usually unconstricted on M3, and limbs short and robust with respect to other representatives of the genus. Further differs from its sister subspecies, *C. a. praecursor*, in having a infraorbital foramen located above molars, a base of the zygomatic process maxillary low, an articular tubercle of the squamosal with a concave profile, a protocone usually unconstricted on M1-2, and an entoconid constricted on lower cheek teeth (Fig. 9).

Coelodonta antiquitatis praecursor Guérin, 1980: Less derived representative of *C. antiquitatis*, defined by a infraorbital foramen located above premolars, a base of the zygomatic maxillary process high, a postorbital process present on the zygomatic arch, an articular tubercle of the squamosal with a straight profile, a protocone unconstricted on M1-2, and an entoconid joined to the hypolophid on lower cheek teeth (Fig. 9). Further differs from the

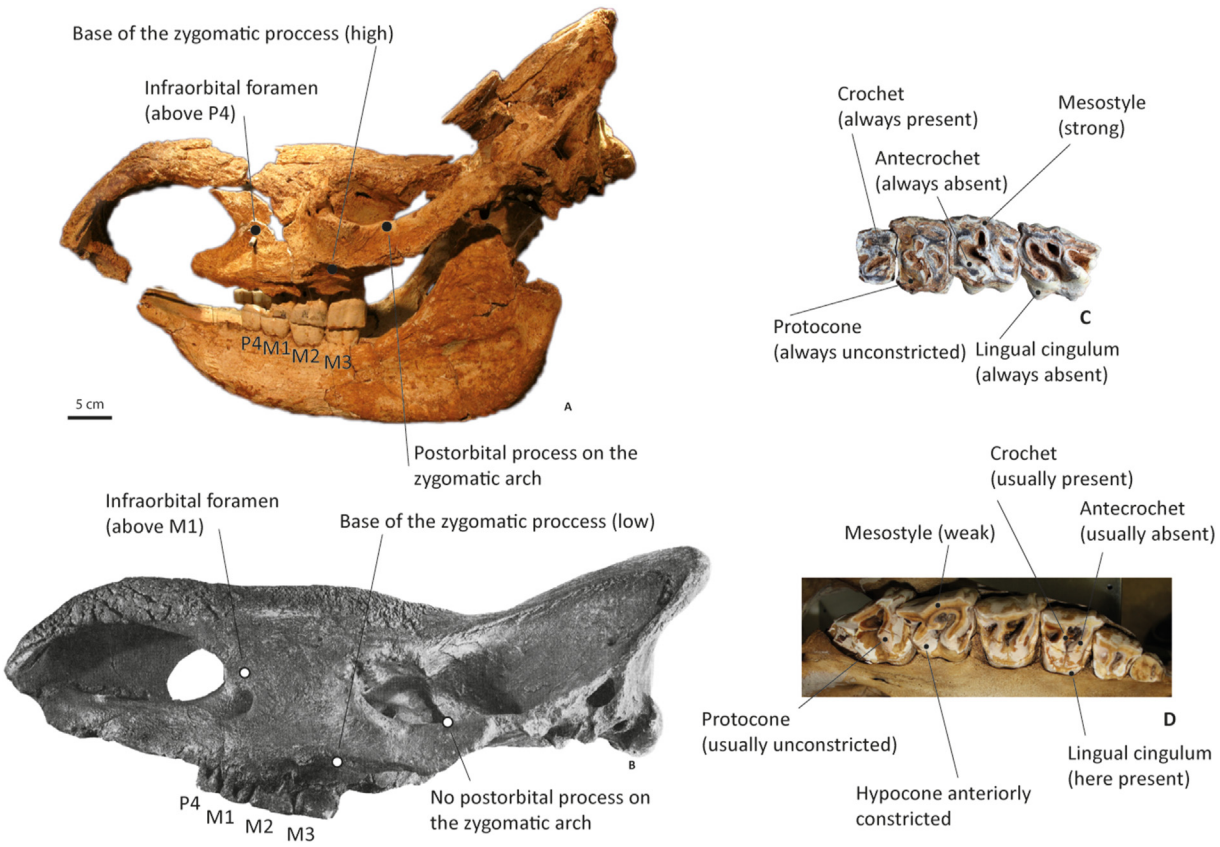

Fig. 9. Illustration of some anatomical differences between *C. a. praecursor* (A and C) and *C. a. antiquitatis* (B and D). A and C: *C. a. praecursor* skull and left upper teeth row (with P4, M1, M2 and M3) from Les Rameaux (this study); B: *C. a. antiquitatis* skull from Jaurens (Guérin, 1983); D: *C. a. antiquitatis* upper right maxillary (with M3 to P2) from Wasserbillig (Luxembourg, Late Pleistocene), illustrative photo courtesy of M. Fabre.

nominal subspecies, *C. a. antiquitatis*, in possessing a crochet always present and a lingual cingulum always absent on P2-4 and upper molars, an antecrochet always absent on P2-3, P4, and upper molars, D1/P1 always absent, a hypocone unconstricted on M1 and M2, antecrochet and hypocone always separate on M1, a mesostyle strong on M2, a protocone always unconstricted on M3, limbs long and slender, a skull with narrow occipital condyles indicator of a less low head carriage in comparison with *C. a. antiquitatis*.

5. Discussion

The morphometrical analysis of the material, skull and mandible, from Les Rameaux allows us to bring them closer together to the material from La Fage and Romain-la-Roche. It highlights a mixture of primitive and derived morphometric characters on both the skull and teeth and places it in an intermediate position between the Tologoj and Late Pleistocene woolly rhinoceroses, as already distinguished under the name *C. a. praecursor* by Guérin (1980).

In both phylogenetic analyses, the topology of rhinocerotines strongly recalls that of molecular-based analyses of living and recently-extinct rhinoceroses by Cappellini et al. (2019) and Liu et al. (2021), with *Dicerorhinus*, *Stephanorhinus* (*sensu stricto*) and *Coelodonta* close one to another in the favored tree. The phylogenetic relationships of *Coelodonta* terminals are fully consistent with their stratigraphical order of appearance. In both cases, *Coelodonta tologoijensis* and *Coelodonta antiquitatis* are quite distinct. Within the clade *C. antiquitatis*, the two subspecies *C. a. praecursor* and *C. a. antiquitatis* are also separated. The rhinos from Les Rameaux and Bad Frankenhausen are clustering with *C. a. praecursor*.

The metric analysis indicates an intermediate position between *Coelodonta a. antiquitatis* and *C. tologoijensis*: the proportional width of the occipital condyles of Middle Pleistocene *Coelodonta* specimens (La Fage, Romain-la-Roche, Les Rameaux and Bad Frankenhausen) appear to be weaker than in the Late Pleistocene ones (Jaurens, Ajoie, and Arroyo Culebro skull A). In rhinocerotids, grazing specialist species tend to have very strong occipital condyles (Zeuner, 1934; Pandolfi and Maiorino, 2016), perhaps related to their neck musculature and low head carriage (Zeuner, 1934; Borsuk-Bialynicka, 1973). Associated with the weak angulation of the skull between its base and the occipital crest, it indicates a highest head carriage compared to Late Pleistocene *Coelodonta*. However, the proportion of the teeth are neither comparable to *C. tologijensis* nor to *C. a. antiquitatis*. but seems to express a compromise between the two conformations. Guérin (1983) noticed a size reduction of the lower teeth for *Coelodonta* with respect to cranial dimensions over time. This observation may be related to an evolution of the general shape of *Coelodonta* lower premolars over time from rectangular for *C. tologoijensis*, to square on the premolar of the western European *Coelodonta* since the Middle Pleistocene (Les Rameaux, La Fage, Coudoulous II, Romain-la-Roche, and Jaurens).

These characters are clearly and easily observable and mark a chronological step in the supposed linear evolution of *Coelodonta*. Indeed, over time, this genus appears to become increasingly short-legged, robust, and with a lower head carriage (Guérin, 1980; Tong and Wang, 2014; Deng et al., 2011). This chronological evolutionary trajectory/trend is accompanied by a geographical pathway with a

spread from Tibet (Deng et al., 2011) to China (Guo et al., 2002), Russia, and Mongolia (Vangengejm et al., 1966; Bazarov et al., 1976; Vangenheim and Sotokova, 1981) and then to western Europe (Guérin, 1973; Kahlke and Lacombat, 2008). According to this study, *C. tologoijensis* does not exist in Europe and, pending further discoveries, its expansion seems to be confined/limited to Russia and Mongolia. Only the species *C. antiquitatis* is represented in Europe with two chronologically succeeding subspecies: *C. a. praecursor* and *C. a. antiquitatis*. This taxon would have been highly adapted to cold climates (Boeskorov, 2012; Lord et al., 2020) and oriented toward the consumption of low plants (Stefaniak et al., 2021) but nevertheless capable of eco-ethological flexibilities (Rivals et al., 2009; Rey-Iglesia et al., 2021). The less specialized anatomy of *C. a. praecursor* may reflect even greater ecological flexibility compared to the more recent subspecies.

6. Conclusions

Four species are here recognized within the genus *Coelodonta*. *Coelodonta thibetana* is the earliest representative (late Pliocene), then *C. nihowanensis* (Early–Middle Pleistocene) occurs, and finally two more derived forms occur, with *C. tologoijensis* (Middle Pleistocene) and *C. antiquitatis* (Middle–Late Pleistocene). This latter species can be divided into two chrono-subspecies: *C. a. praecursor* (Middle Pleistocene) and *C. a. antiquitatis* (Late Pleistocene). The latter subspecies is the animal depicted in cave or portable art by upper Paleolithic human groups.

In agreement with Guérin (2010), we consider that all European fossil specimens of *Coelodonta* can be confidently assigned to *C. antiquitatis*. Our analyses, based on the Les Rameaux's skull, allow us to consider *C. a. praecursor* Guérin, 1980 as a valid subspecies and to describe more precisely its characteristics. This Middle Pleistocene subspecies is also recorded in France (La Fage, Romain-la-Roche, and Coudoulous II), Germany (e.g. Bad Frankenhausen) and possibly in Greece (Gephyra). Even through it is beyond the scope of the current work, a thorough revision of Middle Pleistocene Chinese representatives of *Coelodonta* shall be undertaken, especially in the light of the current results.

Authors contribution

Antigone Uzunidis: Conceptualization, Methodology, Formal analysis, Investigation, Writing – original draft, Writing – review & editing, Visualization. **Pierre-Olivier Antoine**: Methodology, Formal analysis, Investigation, Writing – original draft, Writing – review & editing. **Jean-Philip Brugal**: Investigation, Resources, Writing – original draft, Writing – review & editing.

Declaration of competing interest

The authors declare that they have no known competing financial interests or personal relationships that could have appeared to influence the work reported in this paper.

Acknowledgements

Excavations of Les Rameaux were made by the late François Rouzaud, funded by SRA Midi-Pyrénées, and one of us (JPB who actively participated in the fieldwork) would like to express his great emotion and friendship in honor of F. Rouzaud. We are deeply indebted to Alexander Sizov (Institute of the Earth's Crust of the Russian Academy of Sciences, Irkustk) for providing invaluable literature and sharing his knowledge on the Transbaikalian Pleistocene fossil record. The morphometric study was carried out by AU while she was in the laboratory of LAMPEA, UMR 7269, to whom she would like to express her warm thanks here. The authors thanks deeply Magali Fabre (Antea Archéologie) who provide the photo of the maxillary of a Late Pleistocene *Coelodonta*. Also, the authors would like to express their gratitude to the two anonymous reviewer who were very helpful in improving the manuscript.

Appendix A. Supplementary data

Supplementary data to this article can be found online at https://doi.org/10.1016/j.quascirev.2022.107594.

References

Alexeeva, N., Erbajeva, M., 2005. Changes in the fossil mammal faunas of western transbaikalia during the pliocene–pleistocene boundary and the early–middle Pleistocene transition. Quat. Int. 131, 109–115. https://doi.org/10.1016/j.quaint.2004.07.002.

Álvarez-Lao, D.J., García, N., 2011. Southern dispersal and Palaeoecological implications of woolly rhinoceros (Coelodonta antiquitatis): review of the Iberian occurrences. Quat. Sci. Rev. 30, 2002–2017. https://doi.org/10.1016/j.quascirev.2011.05.005.

Antoine, P.-O., 2002. Phylogénie et évolution des Elasmotheriina (Mammalia, Rhinocerotidae), Mémoires du Muséum national d'Histoire naturelle. Publications scientifiques du Muséum, Paris.

Antoine, P.-O., 2003. Middle Miocene elasmotheriine Rhinocerotidae from China and Mongolia: taxonomic revision and phylogenetic relationships. Zool. Scripta 32, 95–118.

Antoine, P.-O., Reyes, M.C., Amano, N., Bautista, A.P., Chang, C.-H., Claude, J., De Vos, J., Ingicco, T., 2022. A new rhinoceros clade from the Pleistocene of Asia sheds light on mammal dispersals to the Philippines. Zool. J. Linnean Soc. 194 (2), 416–430. https://doi.org/10.1093/zoolinnean/zlab009.

Antoine, P., Sarac, G., 2005. Rhinocerotidae (mammalia, Perissodactyla) from the late Miocene of akkasdagi, Turkey. Geodiversitas 274, 601–632.

Antoine, P.-O.. in press. Rhinocerotids from the Siwalik faunal sequence. In: Badgley, C., Pilbeam, D. & Morgan, M. (eds.), At the Foot of the Himalayas: Paleontology and Ecosystem Dynamics of the Siwalik Record of Pakistan. Johns Hopkins University Press.

Antoine, P.-O., Downing, K.F., Crochet, J.-Y., Duranthon, F., Flynn, L.J., Marivaux, L., Métais, G., Rajpar, A.R., Roohi, G., 2010. A revision of aceratherium blanfordi lydekker, 1884 (mammalia: Rhinocerotidae) from the early Miocene of Pakistan: postcranials as a key. Zool. J. Linn. Soc. 160, 139–194. https://doi.org/10.1111/j.1096-3642.2009.00597.x.

Argant, A., Brugal, J.-P., 2017. The cave lion Panthera (Leo) spelaea and its evolution: Panthera spelaea intermedia nov. subspecies. Acta Zool. Cracov. 60, 58–103. https://doi.org/10.3409/azc.60_2.59.

Arsuaga, P.M., Aguirre, E., 1979. Rinocerontes lanudos en la provincia de Madrid (Coelodonta antiquitatis Blumenbach). Bol. Real Soc. Espanola Hist. Nat. Secc. Geol. 77, 23–59.

Bautista, A.P., 1995. Fossil remains of rhinoceros from the Philippines. National Museum Papers 5, 1–9.

Bazarov, D.B., Erbajeva, M., Rezanov, I.N., 1976. Geology and Fauna of Reference Sections of Anthropogenic Deposits of Western Transbaikalia. Nauka, Moscow (in russian).

Becker, D., Antoine, P.-O., Maridet, O., 2013. A new genus of Rhinocerotidae (mammalia, Perissodactyla) from the oligocene of Europe. J. Syst. Palaeontol. 11, 947–972. https://doi.org/10.1080/14772019.2012.699007.

Becker, D., Dini, M., Scherler, L., 2015. Rhinocéros laineux du Pléistocène supérieur d'Ajoie (Canton du Jura Suisse) : description anatomique et implications écologiques. Rev. Paléobiol. 34, 27–44.

Blumenbach, J.F., 1799. Handbuch der Naturgeschichte. Dieterich, Göttingen.

Boeskorov, G.G., 2012. Some specific morphological and ecological features of the fossil woolly rhinoceros (Coelodonta antiquitatis Blumenbach 1799). Biol. Bull. 39, 692–707.

Boivin, M., Marivaux, L., Antoine, P.-O., 2019. L'apport du registre paléogène d'Amazonie sur la diversification initiale des Caviomorpha (Hystricognathi, Rodentia): implications phylogénétiques, macroévolutives et paléobiogéographiques. geod 41, 143–245. https://doi.org/10.5252/geodiversitas2019v41a4.

Bonifay, M.-F., 1967. Principales formes caractéristiques du Quaternaire moyen du sud-est de la France (Grands Mammifères). Bull. Musee Anthropol. Prehist. Monaco 14, 49–62.

Bonifay, M.-F., 1971. Carnivores quaternaires du sud-est de la France (Unpublised "these d'état"). Paris Faculty of Science, Paris.

Borsuk-Bialynicka, M., 1973. Studies on the pleistocène rhinocéros Coelodonta antiquitatis (Blumenbach). Acta Palaeontologia Polonica 29, 1–94.

Boudadi-Maligne, M., 2010. Les canis pléistocènes du sud de la France approche biosystématique, évolutive et biochronologique (unpublished PhD). Bordeaux 1 university.

Boudadi-Maligne, M., 2012. Une nouvelle sous-espèce de loup (Canis lupus maximus nov. subsp.) dans le Pléistocène supérieur d'Europe occidentale. Comptes Rendus Palevol 11, 475–484. https://doi.org/10.1016/j.crpv.2012.04.003.

Bourguignon, L., Crochet, J.-Y., Capdevila, R., Ivorra, J., Antoine, P.-O., Agustí, J., Barsky, D., Blain, H.-A., Boulbes, N., Bruxelles, L., Claude, J., Cochard, D., Filoux, A., Firmat, C., Lozano-Fernández, I., Magniez, P., Pelletier, M., Rios-Garaizar, J., Testu, A., Valensi, P., De Weyer, L., 2016. Bois-de-Riquet (Lézignan-la-Cèbe, Hérault): a late early Pleistocene archeological occurrence in southern France. Quaternary International, The first peopling of Europe and technological change during the Lower-Middle Pleistocene transition 393, 24–40. https://doi.org/10.1016/j.quaint.2015.06.037.

Bronn, H.G., 1831. Italiens Tertiär-Gebilde und deren organische Einschlüsse: vier Abhandlungen. Groos, Heidelberg, Germany. https://doi.org/10.5962/bhl.title.59236.

Brugal, J.-P., Jaubert, J., 1991. Les gisements paléontologiques pléistocènes à indices de fréquentation humaine : un nouveau type de comportement de prédation. Paléo 3, 15–41.

Brugal, J.-P., Giuliani, C., Fosse, P., Fourvel, J.-B., Magniez, P., Pelletier, M., Uzunidis, A., 2021. Preliminary data on the Middle Pleistocene site of Lunel viel I (Hérault, France). Alpine and Mediterranean Quaternary 34, 1–13. https://doi.org/10.26382/AMQ.2021.08.

Cappellini, E., Welker, F., Pandolfi, L., Ramos-Madrigal, J., Samodova, D., Rüther, P.L., Fotakis, A.K., Lyon, D., Moreno-Mayar, J.V., Bukhsianidze, M., Rakownikow Jersie-Christensen, R., Mackie, M., Ginolhac, A., Ferring, R., Tappen, M., Palkopoulou, E., Dickinson, M.R., Stafford, T.W., Chan, Y.L., Götherström, A., Nathan, S.K.S.S., Heintzman, P.D., Kapp, J.D., Kirillova, I., Moodley, Y., Agusti, J., Kahlke, R.-D., Kiladze, G., Martínez-Navarro, B., Liu, S., Sandoval Velasco, M., Sinding, M.-H.S., Kelstrup, C.D., Allentoft, M.E., Orlando, L., Penkman, K., Shapiro, B., Rook, L., Dalén, L., Gilbert, M.T.P., Olsen, J.V., Lordkipanidze, D., Willerslev, E., 2019. Early Pleistocene enamel proteome from Dmanisi resolves Stephanorhinus phylogeny. Nature 574, 103–107. https://doi.org/10.1038/s41586-019-1555-y.

Cerdeño, E., 1995. Cladistic analysis of the family Rhinocerotidae (Perissodactyla). Am. Mus. Novit. 3142, 1–25.

Coumont, M.-P., 2006. Taphonomie préhistorique : mammifères fossiles en contexte d'avens pièges. Apport pour l'étude des archeofaunes. Aix-Marseille I university, Aix-en Provence (Unpublished PhD).

Croitor, R., Bonifay, M.-F., Brugal, J.-P., 2008. Systematic revision of the endemic deer Haploidoceros n. gen. Mediterraneus (Bonifay, 1967) (mammalia, cervidae) from the Middle Pleistocene of southern France. Paläontol. Z. 82, 325–346. https://doi.org/10.1007/BF02988899.

Daura, J., Sanz, M., Julià, R., García-Fernández, D., Fornós, J.J., Vaquero, M., Allué, E., López-García, J.M., Blain, H.A., Ortiz, J.E., Torres, T., Albert, R.M., Rodríguez-Cintas, À., Sánchez-Marco, A., Cerdeño, E., Skinner, A.R., Asmeron, Y., Polyak, V.J., Garcés, M., Arnold, L.J., Demuro, M., Pike, A.W.G., Euba, I., Rodríguez, R.F., Yagüe, A.S., Villaescusa, L., Gómez, S., Rubio, A., Pedro, M., Fullola, J.M., Zilhão, J., 2015. Cova del Rinoceront (Castelldefels, Barcelona): a terrestrial record for the Last Interglacial period (MIS 5) in the Mediterranean coast of the Iberian Peninsula. Quat. Sci. Rev. 114, 203–227. https://doi.org/10.1016/j.quascirev.2015.02.014.

Deng, T., Wang, X., Fortelius, M., Li, Q., Wang, Y., Tseng, Z.J., Takeuchi, G.T., Saylor, J.E., Säilä, L.K., Xie, G., 2011. Out of Tibet: Pliocene woolly rhino suggests high-pLateau origin of Ice Age megaherbivores. Science 333, 1285–1288.

Eisenmann, V., Kuznetsova, T., 2004. Early Pleistocene equids (mammalia, Perissodactyla) of nalaikha, Mongolia, and the emergence of modern Equus linnaeus, 1758. Geodiversitas 26, 535–561.

Fourvel, J.-B., Fosse, P., Fernandez, P., Antoine, P.-O., 2014. La grotte de Fouvent, dit l'Abri Cuvier (Fouvent-le-Bas, Haute-Saône, France) : analyse taphonomique d'un repaire d'hyènes du Pléistocène supérieur (OIS 3). Paléo 25, 79–99.

Giaourtsakis, I.X., 2022. The fossil record of rhinocerotids (mammalia: Perissodactyla: Rhinocerotidae) in Greece. In: Vlachos, E. (Ed.), Fossil Vertebrates of Greece Vol. 2: Laurasiatherians, Artiodactyls, Perissodactyls, Carnivorans, and Island Endemics. Springer, Cham, pp. 409–500. https://doi.org/10.1007/978-3-030-68442-6_14.

Groves, C.P., 1983. Phylogeny of the living species of Rhinoceros. J. Zool. Syst. Evol. Res. 21, 293–313. https://doi.org/10.1111/j.1439-0469.1983.tb00297.x.

Guérin, C., 1973. Les trois espèces de rhinocéros (Mammalia, Perissodactyla) du gisement pléistocène moyen des Abîmes de La Fage à Nouailles (Corrèze). Nouv. Arch. Mus. Hist. Nat. Lyon 11, 55–84.

Guérin, C., 1980. Les Rhinocéros (Mammalia, Perissodactyla) du Miocène terminal au Pleistocène superieur en Europe occidentale. Comparaison avec les espèces actuelles. Univ. Claude-Bernard, Département des Sciences de la Terre, Lyon (Unpublished PhD).

Guérin, C., 1983. Le gisement pléistocène supérieur de la grotte de Jaurens à Nespouls, Corrèze, France : Les Rhinocerotidae (Mammalia, Perissodactyla). Nouv. Arch. Mus. Hist. Nat. Lyon 21, 65–85.

Guérin, C., 2010. Coelodonta antiquitatis praecursor (Rhinocerotidae) du Pléistocène moyen final de l'aven de Romain-la-Roche (Doubs, France). Rev. Paleobiol. 29, 697–746.

Guo, Z.T., Ruddiman, W.F., Hao, Q., Wu, H.B., Qiao, Y.S., Zhu, R.X., Peng, S.Z., Wei, J.J., Yuan, B.Y., Liu, T.S., 2002. Onset of Asian desertification by 22 Myr ago inferred from loess deposits in China. Nature 416, 159–163.

Guthrie, R.D., 1990. Late Pleistocene faunal revolution. A new perspective on the extinction debate. In: Agenbroad, L.D., Mead, J.I., Nelson, L.W. (Eds.), Megafauna & Man: Discovery of America's Heartland. Mammoth Site of Hot Springs. South Dakota, Inc.; Northern Arizona University, Hot Springs, Arizona, America, pp. 42–60.

Heissig, K., 1972. Palaontologische und geologische Untersuchungen im Tertiar von Pakistan 5. Rhinocerotidae (Mamm.) aus den unteren und mittleren Siwalik-Schichten. Abhandlungen der Bayerischen Akademie der Wissenschaften. Mathematisch-naturwissenschaftliche Klasse, München, Germany.

Heissig, K., 1999. Familly Rhinocerotidae. In: Rössner, G.E., Heissig, K. (Eds.), The Miocene Land Mammals of Europe. Pfeil, pp. 175–188.

Heissig, K., 2012. Les Rhinocerotidae (Perissodactyla) de Sansan. Mémoires du Muséum national d'histoire naturelle, Paris, p. 169.

Ingicco, T., Bergh van den, GD, Jago-on, C., Bahain, J.J., Chacón, M.G., Amano, N., Forestier, H., King, C., Manalo, K., Nomade, S., Pereira, A., Reyes, M.C., Sémah, A.M., Shao, Q., Voinchet, P., Falguères, C., Albers, P.C.H., Lising, M., Lyras, G., Yurnaldi, D., Rochette, P., Bautista, A., Vos de, J, 2018. Earliest known hominin activity in the Philippines by 709 thousand years ago. Nature 557, 233.

Jeannet, M., 2005. La microfaune de l'Igue des Rameaux à Saint-Antonin-Noble-Val (Tarn-et-Garonne, France). Essai de Biostratigraphie. Bulletin de Préhistoire du Sud-Ouest 12, 109–125.

Jeannet, M., Mein, P., 2016. Les Muridae (Mammalia, Rodentia) du Pléistocène moyen de l'Igue des Rameaux (Tarn-et-Garonne, France). Paléo 27, 177–205.

Kahlke, H.D., 1969. Die Rhinocerotiden-Reste aus den Kiesen von Süßenborn bei Weimar. Paläontologische Abhandlungen A III, 667–708.

Kahlke, R.-D., 1994. Die Entstehungs-, Entwicklungs- und Verbreitungsgeschichte des oberpleistozänen Mammuthus-Coelodonta-Faunenkomplexes in Eurasien (Grosssäuger). W. Kramer, Frankfurt.

Kahlke, R.-D., 1999. The History of the Origin, Evolution and Dispersal of the Late Pleistocene Mammuthus-Coelodonta Faunal Complex in Eurasia (Large Mammals). Mammoth Site of Hot Springs.

Kahlke, R.-D., 2014. The origin of eurasian mammoth faunas (Mammuthus-Coelodonta faunal complex). Quat. Sci. Rev. 96, 32–49. https://doi.org/10.1016/j.quascirev.2013.01.012.

Kahlke, R.-D., Lacombat, F., 2008. The earliest immigration of woolly rhinoceros (Coelodonta tologoijensis, Rhinocerotidae, Mammalia) into Europe and its adaptive evolution in Palaearctic cold stage mammal faunas. Quat. Sci. Rev. 27, 1951–1961.

Kahlke, R.-D., García, N., Kostopoulos, D.S., Lacombat, F., Lister, A.M., Mazza, P.P.A., Spassov, N., Titov, V.V., 2011. Western Palaearctic palaeoenvironmental conditions during the Early and early Middle Pleistocene inferred from large mammal communities, and implications for hominin dispersal in Europe. Quat. Sci. Rev. 30, 1368–1395. https://doi.org/10.1016/j.quascirev.2010.07.020.

Kalmykov, N.P., 2016. Mammals of the framing of Lake Baikal in the fossil record. Bajkal'skij Zoologiceskij Zhurnal 1, 61–69 ([in Russian, English abstract]).

Kuzmin, Y., 2010. Extinction of the woolly mammoth (Mammuthus primigenius) and woolly rhinoceros (Coelodonta antiquitatis) in Eurasia: review of chronological and environmental issues. Boreas 39, 247–261.

Liu, S., Westbury, M.V., Dussex, N., Mitchell, K.J., Sinding, M.-H.S., Heintzman, P.D., Duchêne, D.A., Kapp, J.D., von Seth, J., Heiniger, H., Sánchez-Barreiro, F., Margaryan, A., André-Olsen, R., De Cahsan, B., Meng, G., Yang, C., Chen, L., van der Valk, T., Moodley, Y., Rookmaaker, K., Bruford, M.W., Ryder, O., Steiner, C., Bruins-van Sonsbeek, L.G.R., Vartanyan, S., Guo, C., Cooper, A., Kosintsev, P., Kirillova, I., Lister, A.M., Marques-Bonet, T., Gopalakrishnan, S., Dunn, R.R., Lorenzen, E.D., Shapiro, B., Zhang, G., Antoine, P.-O., Dalén, L., Gilbert, M.T.P., 2021. Ancient and modern genomes unravel the evolutionary history of the rhinoceros family. Cell 184. https://doi.org/10.1016/j.cell.2021.07.032, 4874-4885.e16.

Lord, E., Dussex, N., Kierczak, M., Díez-del-Molino, D., Ryder, O.A., Stanton, D.W.G., Gilbert, M.T.P., Sánchez-Barreiro, F., Zhang, G., Sinding, M.-H.S., Lorenzen, E.D., Willerslev, E., Protopopov, A., Shidlovskiy, F., Fedorov, S., Bocherens, H., Nathan, S.K.S.S., Goossens, B., van der Plicht, J., Chan, Y.L., Prost, S., Potapova, O., Kirillova, I., Lister, A.M., Heintzman, P.D., Kapp, J.D., Shapiro, B., Vartanyan, S., Götherström, A., Dalén, L., 2020. Pre-extinction demographic stability and genomic signatures of adaptation in the woolly rhinoceros. Curr. Biol. 30. https://doi.org/10.1016/j.cub.2020.07.046, 3871-3879.e7.

van der Made, J., 2010. The rhinos from the Middle Pleistocene of neumark-nord (Saxony-Anhalt). Veröffentlichungen des Landesamtes für Archeologie 62, 432–527.

van der Made, J., Mazo, A., 2014-2015. Los grandes mamíferos del yacimiento de PRERESA, Haploidoceros mediterraneus. Una nueva especie de ciervo en el Pleistoceno Ibérico. Museo Arqueológico Regional, Alcalá de Henares, pp. 39–45.

Orliac, M.J., Pierre-Olivier, A., Ducrocq, S., 2010. Phylogenetic relationships of the suidae (mammalia, cetartiodactyla): new insights on the relationships within suoidea. Zool. Scripta 39, 315–330. https://doi.org/10.1111/j.1463-6409.2010.00431.x.

Orlova, L.A., Kuzmin, Y.V., Dementiev, V.N., 2004. A review of the evidence for extinction chronologies for five species of upper Pleistocene megafauna in siberia. Radiocarbon 46, 301–314.

Otsuka, H., Lin, C.C., 1984. Fossil rhinoceros from the T'ouk'oushan group in taiwan. J. Taiwan Mus. 37, 1–35.

Pandolfi, L., Maiorino, L., 2016. Reassessment of the largest Pleistocene rhinocerotine rhinoceros platyrhinus (mammalia, Rhinocerotidae) from the upper siwaliks (siwalik hills, India). J. Vertebr. Paleontol. 36, e1071266. https://doi.org/10.1080/02724634.2015.1071266.

Pandolfi, L., Gasparik, M., Magyar, I., 2016. Rhinocerotidae from the upper Miocene deposits of the western pannonian basin (Hungary): implications for migration routes and biogeography. Geol. Carpathica 67, 69–82. https://doi.org/10.1515/geoca-2016-0004.

Pandolfi, L., Marra, A., Carone, G., Maiorino, L., Rook, L., 2021a. A new rhinocerotid

(mammalia, Rhinocerotidae) from the latest Miocene of southern Italy. Hist. Biol. 33 (2), 194–208. https://doi.org/10.1080/08912963.2019.1602615.
Pandolfi, L., Antoine, P.-O., Bukhsianidze, M., Lordkipanidze, D., Rook, L., 2021b. Northern eurasian rhinocerotines (mammalia, Perissodactyla) by the pliocene–pleistocene transition: phylogeny and historical biogeography. J. Syst. Palaeontol. 1–27. https://doi.org/10.1080/14772019.2021.1995907.
Pelletier, M., 2018. Évolution morphométrique et biogéographie des Léporidés dans les environnements méditerranéens au Pléistocène. Implications socio-économiques pour les sociétés humaines (Unpublished PhD). Aix-Marseille University, Aix-en Provence.
Puzachenko, A.Y., Kirillova, I.V., Shidlovsky, F.K., Levchenko, V.A., 2021. Variability and morphological features of woolly rhinoceros skulls (Coelodonta antiquitatis (Blumenbach 1799)) from northeastern Asia in the late Pleistocene. Biol Bull Russ Acad Sci 48, S185–S196. https://doi.org/10.1134/S1062359021140144.
Qiu, Z., Wang, B.Y., Deng, T., 2004. Indricotheres (Perissodactyla, mammalia) from oligocene in linxia basin, gansu, China. Vertebr. Palasiat. 42, 177–192.
Rey-Iglesia, A., Lister, A.M., Stuart, A.J., Bocherens, H., Szpak, P., Willerslev, E., Lorenzen, E.D., 2021. Late Pleistocene paleoecology and phylogeography of woolly rhinoceroses. Quat. Sci. Rev. 263, 106993. https://doi.org/10.1016/j.quascirev.2021.106993.
Rivals, F., Schulz, E., Kaiser, T.M., 2009. Late and Middle Pleistocene unguLates dietary diversity in Western Europe indicate variations of Neanderthal paleoenvironments through time and space. Quat. Sci. Rev. 3388–3400.
Rouzaud, F., Soulier, M., Brugal, J.-P., Jaubert, J., 1990. L'igue des Rameaux (Saint-Antonin-Noble-Val, Tarn-et-Garonne). Un nouveau gisement du Pléistocène moyen. Premiers résultats. Paléo 2, 89–106.
Shpansky, A.V., Boeskorov, G.G., 2018. Northernmost Record of the Merck's Rhinoceros Stephanorhinus kirchbergensis (Jäger) and Taxonomic Status of Coelodonta jacuticus Russanov (Mammalia, Rhinocerotidae). Paleontol. J. 52 (4), 445–462. https://doi.org/10.1134/S003103011804010X.
Simpson, G.G., 1941. Large Pleistocene Felines of North America, American Museum Novitates. American Museum of Natural History, New York City.
Stefaniak, K., Stachowicz-Rybka, R., Borówka, R.K., Hrynowiecka, A., Sobczyk, A., Moskal-del Hoyo, M., Kotowski, A., Nowakowski, D., Krajcarz, M.T., Billia, E.M.E., Persico, D., Burkanova, E.M., Leshchinskiy, S.V., van Asperen, E., Ratajczak, U., Shpansky, A.V., Lempart, M., Wach, B., Niska, M., van der Made, J., Stachowicz, K., Lenarczyk, J., Piątek, J., Kovalchuk, O., 2021. Browsers, grazers or mix-feeders? Study of the diet of extinct Pleistocene Eurasian forest rhinoceros Stephanorhinus kirchbergensis (Jäger, 1839) and woolly rhinoceros Coelodonta antiquitatis (Blumenbach, 1799). Quat. Int. 192–212. https://doi.org/10.1016/j.quaint.2020.08.039.
Stuart, A.J., Lister, A.M., 2007. Patterns of late quaternary megafaunal extinctions in Europe and northern Asia. Cour. Forschungsinst. Senckenberg 287–297.
Swofford, D.L., 2001. PAUP^*: Phylogenetic Analysis Using Parsimony (And Other Methods) 4.0 B8. Sinauer, Sunderland, MA.
Tissier, J., Antoine, P.-O., Becker, D., 2021. New species, revision, and phylogeny of Ronzotherium aymard, 1854 (Perissodactyla, Rhinocerotidae). European Journal of Taxonomy 753, 1–80. https://doi.org/10.5852/ejt.2021.753.1389.
Tong, H., Guérin, C., 2009. Early Pleistocene Dicerorhinus sumatrensis remains from the liucheng gigantopithecus cave, guangxi. Geobios 525–539.
Tong, H.-W., Hu, N., Han, F., 2011. A preliminary report on the excavations at the early Pleistocene fossil site of shanshenmiaozui in nihewan basin, hebei, China. Quat. Sci. 31, 643–653 [Chinese 643–652; English 653].
Tong, H.-W., Wang, X.-M., 2014. Juvenile skulls and other postcranial bones of Coelodonta nihowanensis from Shanshenmiaozui, Nihewan Basin, China. J. Vertebr. Paleontol. 34, 710–724. https://doi.org/10.1080/02724634.2013.814661.
Tsoukala, E., 1991. A Coelodonta antiquitatis praecursor (mammalia, Rhinocerotidae, zone 24) from the axios valley deposits (Gephyra, Macedonia, N. Greece). Bull. Geol. Soc. Greece 25, 473–485.
Uzunidis-Boutillier, A., 2017. Grands herbivores de la fin du Pléistocène moyen au début du Pléistocène supérieur dans le sud de la France. Implications anthropologiques pour la lignée néandertalienne. Aix-Marseille University, Aix-en Provence (Unpublished PhD).
Uzunidis, A., Brugal, J.-P., 2018. Les grands herbivores (Bovinés, Équidés, Rhinocérotidés, Proboscidiens) de la fin du Pléistocène Moyen: la couche 9 de Coudoulous II (Lot, Quercy, Sud-Ouest France). Paléo 29, 223–249.
Vangengejm, E.A., Belyaeva, E.I., Garutt, V.E., Dmitrieva, E.I., Zazhigin, V.S., 1966. Mlekopitayushchie Eopleistocena Zapadnogo Zabaikal'ya. Nauka, Moskva.
Vangengejm, E.A., Sotokova, M.V., 1981. Geology and mammal fauna of the site of dasukhino, western zabaykalia (in Russian). Newsletter of the Quaternary Research Commission 56, 106–117.
Yan, Y., Wang, Y., Jin, C., Mead, J.I., 2014. New remains of rhinoceros (Rhinocerotidae, Perissodactyla, mammalia) associated with gigantopithecus blacki from the early Pleistocene yanliang cave, fusui, South China. Quat. Int. 354, 110–121.
Zeuner, F., 1934. Die Beziehungen zwischen Schädelform und Lebensweise bei den rezenten und fossilen Nashörnern. Berichte des Naturforschenden Gesellschaft zu Freiburg 34, 21–80.